ISTANBUL TECHNICAL UNIVERSITY ★ GRADUATE SCHOOL OF SCIENCE ENGINEERING AND TECHNOLOGY

EFFECT OF PARTICLE MORPHOLOGY ON FLOTATION

PhD THESIS

Onur GÜVEN

Department of Mineral Processing Engineering

Mineral Processing

AUGUST 2016

ISTANBUL TECHNICAL UNIVERSITY ★ GRADUATE SCHOOL OF SCIENCE ENGINEERING AND TECHNOLOGY

EFFECT OF PARTICLE MORPHOLOGY ON FLOTATION

PhD THESIS

Onur GÜVEN
(505092005)

Department of Mineral Processing Engineering

Mineral Processing

Thesis Advisor: Prof. Dr. Mehmet Sabri ÇELİK

AUGUST 2016

İSTANBUL TEKNİK ÜNİVERSİTESİ ★ FEN BİLİMLERİ ENSTİTÜSÜ

TANE MORFOLOJİSİNİN FLOTASYONA ETKİSİ

DOKTORA TEZİ

Onur GÜVEN
(505092005)

Cevher Hazırlama Mühendisliği

Cevher Hazırlama Programı

Tez Danışmanı: Prof. Dr. Mehmet Sabri ÇELİK

AĞUSTOS 2016

Onur Güven, a Ph.D. student of İTU Graduate School of Science Engineering and Technology student ID 505092005, successfully defended the thesis/dissertation entitled "EFFECT OF PARTICLE MORPHOLOGY ON FLOTATION", which he prepared after fulfilling the requirements specified in the associated legislations, before the jury whose signatures are below.

Thesis Advisor : **Prof. Dr. Mehmet Sabri Çelik**
İstanbul Technical University

Jury Members : **Prof. Dr. Ayhan Ali SİRKECİ**
Istanbul Technical University

Prof. Dr. Mehmet POLAT
İzmir Institute of Technology

Prof. Dr. Gülay BULUT
Istanbul Technical University

Assoc. Prof. Dr. Orhan ÖZDEMİR
Istanbul University

Date of Submission : 19 July 2016
Date of Defense : 09 Aug 2016

To my family,

FOREWORD

This thesis would not be possible without the guidance, support and generous contribution of many people. It is my pleasure to thank to those who made this possible. First of all, my special thanks to my advisor Prof. Dr. Mehmet Sabri Celik for his kind guidance, support and encouragement throughout my scientific studies and my whole life. And also being a member of "Surface Chemistry" team provided me all the facilities and all the equipment to continue my studies. And thanks to all thesis commettee and juries Prof. Dr. Ayhan Ali Sirkeci, Prof. Dr. Mehmet Polat for their kind suggestions for my PhD study. I would also like to acknowledge the special contribution of Assoc. Prof. Dr. Orhan Ozdemir who always encourage me at all conditions to continue my studies and improve my skill of writing articles with his kind suggestions. My special thanks to Prof. Dr. Fatma Arslan for her kind support and encouragement throughout my life in ITU. And thanks to all Mineral Processing Engineering Department and Mining Faculty staff, it was a great honor to be a member of this department and faculty and Istanbul Technical University.
In addition, I would like to thank to all "Surface Innovation" team and all staff in MTU for funny and joyfull memories during my experiments and my whole life in USA. But my special thanks to Prof. Dr. Jaroslaw W. Drelich for guiding throughout all my studies both experimentally and theoretically and to provide me a new scientific point of view for my academic life. I would also like to thank to Assoc. Prof. Dr. Fırat Karakas and Dr. Ethem Karaagaclioglu, MSc. Behzad Vaziri Hassas, Mrs. Nurgül Kodrazi, Mrs. Bala Ekinci Şans, for their kind support during my studies. And special thanks to all my friends, this thesis won't be possible without the funny joyful moments I shared with them. And to my wonderful family for their endless support and absolute confidence in my ability during my life.

I would also like to specially thank to TÜBİTAK 2214A Scholarship program for financially supporting my life and studies in Michigan Technological University, USA.

August 2016

Onur GÜVEN
(Mining Engineer)

TABLE OF CONTENTS

Page

LIST OF TABLES

Page

LIST OF FIGURES

Page

EFFECT OF PARTICLE MORPHOLOGY ON FLOTATION

SUMMARY

Today, due to the finer liberation sizes of minerals, mineral processing methods utilizing the wettability differences of particles like flotation has become more preferable than other methods. Although many individual parameters in flotation process like pH, surfactant type have been explained in detail in many papers, the effect of morphology on flotation recoveries has not been dwelled much. Particularly, the mechanism responsible for the effect of shape and roughness on flotation grade and recoveries requires a thorough systematic studies in order to reveal the extent of bubble particle interactions upon changes in morphology.

It is therefore the aim of this PhD thesis study, to investigate these still questionable and yet still misunderstood phenomenon of particle morphology on flotation recoveries from the persepective of both experimental and theoretical issues and extend the findings to practical industrial roadmaps.

In the experimental part of the thesis, the surface roughness of the particles was monitored with different methods such as acid etching in the presence of HF, grinding in different media (ball and autogenously grinding with very fine sized abrasive) and sand blasting. Among them, sand blasting is probably the most unique. In the literature, sand blasting is generally used for surface etching by blasting of sand sized particles to the surfaces. However, in this study, the morphological changes of particles was investigated by changing the distance between plate–gun and the nozzle pressure. The size distributions of particles, shape factor and roughness of these particles was determined by image analysis method for each fraction upon grinding and sand-blasting processes. The roughness parameter was determined by different methods as B.E.T., optical profilometer, atomic force microscopy (A.F.M.) and scanning electron microscopy (SEM). After morphological characterization of particles, certain fractions (150-106 μm) was subjected to systematic micro-flotation tests. In addition, contact angle measurements were also performed for materials produced under different conditions.

The results of these various tests showed that the selection of particle production method is most critical to assess the particle morphology in terms of roughness and shape factor. It is clearly shown that angular particles always float better than round particles using both flotation and bubble-particle attachment tests. On the other hand, comparison of smooth-spherical and rough-spherical particles identified that roughness is the major parameter determining the flotation rates. In this context, increasing the roughness degree resulted in higher flotation rates, which well correlated with the theoretical models. The results of flotation studies showed that the influence of morphology in terms of shape factor and roughness varied with the hydrophobicity of particles. In other words, at high reagent concentrations, while the shape factor became dominant, at lower hydrophobicities, particle roughness became

the major driving force in the evaluation of flotation recoveries. From this point of view, it is proposes that tuning the particle morphology is of significant importance for industrial applications.

In the theoretical part of the study, a derivative of DLVO theory was adapted from the literature and in order to explain the flotation results through the interactions between bubbles and particles with only roughness values taken into consideration. As a result, it was shown that the distance of separation increased with increasing the roughness which concamitantly increased the level of particle hydrophobicity.

TANE MORFOLOJİSİNİN FLOTASYONA OLAN ETKİSİ

ÖZET

Cevherlerin mineral serbestleşmesi günümüzde giderek azaldığından dolayı ince boyutlarda mineralleri ayırabilen yöntemler önem kazanmaktadır. İnce boyutlarda ayırma yapabilen flotasyon, tanelerin ıslanabilirlik farklarından faydalandığı için özellikle minerallerinin gravite farkı düşük olan cevher gruplarına daha fazla uygulanmaktadır. Reaktif türü ve pH gibi parametrelerin flotasyon sonuçlarına etkileri literatürde ayrıntılı olarak yer almaktadır. Buna mukabili, tane morfolojisinin flotasyon işlemlerindeki etkileriyle ilgili yayımlanan güncel makaleler haricinde, tane morfolojisini oluşturan şekil ve pürüzlülük gibi faktörlerin flotasyon verimlerine olan etkilerini inceleyen makaleler henüz az sayıda olup önerilen mekanizmalar tam olarak teyid edilememiştir.

Bu doktora tez çalışmasında tane morfolojisindeki değişimlerin flotasyon üzerine olan etkileri gerek deneysel gerekse teorik modeller kullanılarak araştırılmıştır. Tezin deneysel kısmında, tanelerin özellikle pürüzlülük değerlerini değiştirmek amacıyla asitle muamele, farklı ortamlarda öğütme (bilyalı değirmende, ince boyutlu aşındırıcı tozlarla) ve kumlama işlemleri uygulanmıştır. Bu yöntemler içinde en çarpıcı olan kumlama yöntemi endüstride genellikle yüzeylerin temizlenmesi, pürüzlendirilmesi yahut aşındırılmasıyla amacıyla belirli şartlar altında tanelerin yüzeylere gönderilmesi prensibine dayalı olarak işletilmektedir. Yapılan bu işlemler neticesinde yüzeylerde meydana gelen değişimler çok ayrıntılı olarak incelenmiş olsa da, yüzeylere gönderilen tanelerin özellikleri hakkında bir çalışma literatürde yer almamaktadır. Dolayısıyla bu çalışmada kumlama işlemleri sonrasında tane yüzeylerinde meydana gelen değişimler tane-yüzey arasındaki mesafenin ve nozül basıncının değişiminin bir fonksiyonu olarak incelenmiştir. Deneylerde öğütme şartları ve kumlama sonrasında elde edilen ürünler için tanelerin boyut dağılımları, şekil faktörleri ve pürüzlülük dereceleri ayrı ayrı yapılmıştır. Literatüre yapılan bu katkının haricinde farklı öğütme şartlarında üretilen tanelerin şekil faktörü ve pürüzlülük değerleri öğütme sürelerinin bir fonksiyonu olarak incelenmiştir.

Tanelerin şekil faktörleri binoküler mikroskopla alınan görüntülerin uygun yazılımlarla değerlendirilerek elde edilebilirken, pürüzlülük parametreleri ise B.E.T., optik profilometre ölçümleri ve atomik kuvvet mikroskobu ve taramalı elektron mikroskobu gibi yöntemlerle belirlenmiştir..

Yapılan bu çalışmalarla, tane üretim yönteminin tanelerin morfolojik özellikleri açısından son derece önemli olduğu gösterilmiş olup, istenilen pürüzlülük ve şekil faktörlerinin elde edilmesinde yöntemle birlikte yöntemin uygulanmasında geçerli parametrelerden örneğin nozül basıncı, öğütücü ortam türü, miktarı ve süresi ve tane boyutu gibi parametrelerin de ayrıca değerlendirilmesi gerektiği gösterilmiştir. Deneysel çalışmalardan elde edilen sonuçlar ışığında, orijinalde yuvarlak olan cam küreleriyle gerçekleştirilen çalışmalarda belirli bir öğütme süresine kadar köşelilik parametresinin yükseldiği ancak bu süreden sonraki süre aralıklarında önemli

değişimler elde edilemediği gösterilmiştir. Öğütme işlemleri neticesinde belirli bir pürüzlülük değerine getirilen tanelerin pürüzlülük derecelerinin ayarlanmasında belirli sürelerde aşındırıcı ortamla muamele işlemleri uygulanmış olup, şekil faktörlerinde nispi değişimlerle birlikte pürüzlülük derecelerinde önemli farklar elde edilmiştir.

Farklı pürüzlülük ve şekil faktörlerine sahip tanelerle yürütülen mikro-flotasyon çalışmalarında daha köşeli tanelerin yuvarlak tanelere nazaran daha yüksek verimle kazanıldığı gösterilmiştir. Bu durum flotasyon işlemlerinde şekil faktörlerinin rolünü göstermekte olup, bir diğer deney serisinde ise aynı şekil faktörüne sahip yuvarlak tanelerde flotasyon verimlerinin değerlendirilmesinde pürüzlülüğün belirleyici bir parametre olduğu gösterilmiştir. Ayrıca literatürde ilk defa yer alacak olan tane morfolojisinin hidrofobisiteyle ilişkisinin incelendiği çalışmalarda, düşük kollektör konsantrasyonlarında flotasyon verimlerinde tane pürüzlülüğü daha etkin bir parametre olurken, yüksek konsantrasyonlarda şekil faktörünün daha etkin rol oynadığı gösterilmiştir.

Cam küreleri ile yapılan bu çalışmalara ek olarak endüstriyel bir hammadde olan alüminayla gerçekleştirilen çalışmalarda ise, orijinal hali köşeli olan alümina tanelerinin yine belirli bir öğütme süresine kadar daha köşeli hale geldiği bir değerden sonra ise düşüşler gerçekleştiği gösterilmiştir. Cam kürelere uygulanan benzer akım şeması sonucunda, en yüksek köşelilik değerine ulaşılan öğütme devresinden alınan ürün, aşındırıcı malzemeyle belirli sürelerde muamele edilerek pürüzlülük derecesi değiştirilmiştir. Ancak alüminanın sertlik derecesi ve köşeli yapısı gereğince, gerek şekil faktörlerinde gerekse pürüzlülük derecelerinde elde edilen değişimler cam kürelerinde olduğu gibi geniş bir aralıkda olmamıştır. Zira bu durum flotasyon verimleri açısından da benzer bir eğilim göstermiş olup, flotasyon verimleri arasında nıspi değişimler elde edildiği görülmüştür.

Farklı kollektör konsantrasyonlarında yapılan deneylerde düşük konsantrasyonlarda gerek öğütülmüş gerekse pürüzlü hale getirilmiş tanelerin daha yüksek değerler verdiği ancak bir karşılaştırma yapılması durumunda işlem görmemiş taneler ve pürüzlü tanelerle yapılan flotasyon verimleri arasındaki farkın, benzer şekilde daha köşeli tanelerle yapılan flotasyon verimleri arasındaki farktan daha yüksek olduğunu belirlenmiştir. Yüksek konsantrasyonlarda ise cam kürelerinde de olduğu üzere şekil faktörünün daha belirleyici bir parametre olduğu gösterilmiştir.

Elde edilen bu sonuçlar ışığında yüksek reaktif konsantrasyonlarında şekil faktörünün etkisinin hakim olduğu ancak hidrofobisitenin zayıf olduğu düşük reaktif konsantrasyonlarında flotasyon verimlerinde pürüzlülüğün esas itici güç olduğu bulunmuştur. Bu kapsamda, uygulamalarda tane morfolojisine ince ayar verilerek önemli kazanımlar sağlanılacağı önerilmektedir.

Bu tez kapsamında yer alan teorik çalışmalarda, DLVO teorisinin bir türevi olan bir model literatürden adapte edilerek kullanılmış ve bu çalışmada elde edilen flotasyon sonuçları, tane-kabarcık etkileşimleri ile açıklanmıştır. Model kapsamında değerlendirilen kuvvetler başlıca van der Waals ve elektriksel çift tabaka kuvetleri olup, bu kuvvetlerin hesabında Hamaker sabiti , tane-kabarcık arası mesafe, tane çapı, debye tabakası kalınlığı gibi parametreler kullanılmaktadır. Hesaplamalar öncelikle pürüzsüz yüzeyler için yapılmış olup, sonrasında pürüzlülük parametresinin eklenmesiyle birlikte pürüzlü yüzeyler arasındaki enerji bariyeri hesaplanmıştır. Ayrıca flotasyon şartlarının doğru olarak analiz edilebilmesi amacıyla DLVO harici bir bileşen olan hidrofobik kuvvetlerde eklenmiştir. Hidrofobik kuvvetlerin hesabında literatürde temelde Washburn denklemleri olarak gösterilen ve van Oss teorisinin esas

alındığı formüllerin türevi alınarak deneysel çalışmalarda kullanılan şartlara adapte edilmiştir. Dolayısıyla model bünyesinde enerji bariyerinin hesabında bu üç kuvvetin toplamı kullanılmış olup, elde edilen enerji bariyeri değerleriyle flotasyon kinetiği sonuçları arasında bir korelasyon kurulmaya çalışılmıştır. Sonuç olarak yuvarlarak tanelerde pürüzlülük derecesinin artmasına mukabil yükselen flotasyon verimlerinin yanı sıra flotasyon kinetiği de artmakta, tane-kabarcık arasındaki enerji bariyeri beklenildiği üzere düşme eğilimi göstermektedir. Bu durum deneysel çalışmalardan elde edilen verilerin teorik bulgularla da uyumlu olduğunu teyid etmektedir.

1. INTRODUCTION

Today, the finer liberation sizes of minerals have led most researchers to investigate alternative methods for enriching the valuable minerals associated with the ore body. Accordingly, while most gravity methods are incompatible with finely disseminated ore bodies and some ore types like sulfides, flotation methods have become preferable for selectively separating the valuables from gangue depending on their wettability difference even at ultrafine sizes. Apart from the influence of many factors on flotation processes such as surface energy, increase in surface area, pH of the medium, and other relevant values on suitable reagent combinations, no plausible explanation for the beneficiation of these fines is suggested to their lower or higher recoveries.

Thus, in addition to those well-known process variables, the effect of particle morphology in terms of roughness (surface texture), roundness, elongation ratio, and sphericity should be considered since the geometry of particles provides a pronounced influence on whole interactions occurring on the surfaces during different technological processes such as flotation, agglomeration and coagulation.

Therefore, the distribution of shape factors and roughness along with the particle size come into prominence in many industrial applications while employing various materials in powder form. However, due to the difficulties of the determination of shape factor and roughness simultaneously after all processes in industrial applications, the importance of this parameter still maintains its importance on the characterization of particulate based processes.

In this context, the objective of this thesis was to identify the morphology of particles produced by different methods such as grinding, abrasion, etching and blasting and to determine its influence on flotation results using both experimental and theoretical considerations.

1.1 Main Hypothesis and Sub-Hypothesis

The main hypothesis addressed in this thesis was “Because particle morphology is one of the misunderstood issues for successful flotation and interaction between bubbles, its determination and modeling with various tests including micro-flotation tests are necessary to understand the exact reasons behind this phenomenon”.

The Sub-hypotheses in this research were;

-Besides many shape factors, deviation from roundness is likely to be the driving force at constant reagent concentration in glass bead-amine system.

-Roughness becomes the only driving force if all the particles are spherical.

-Isolation of roughness and shape from each other as a function of reagent concentration or hydrophobicity is important to individually identify each morphological feature.

1.2 Scope Of The Research

In the second part of the the thesis, a variety of experimental techniques including grinding, sand blasting, shape factor and roughness analysis, and micro-flotation tests in quartz-Flotigam EDA (ethylene-diamine) was used to determine the effect of surface morphology on flotation recovery. In the third part, the effects of abrasion and etching on roughness were studied, and the results were explained with the help of flotation tests and theoretical assumptions based on the roughness values measured by AFM. In the forth and fifth parts of the thesis, the isolation of shape factor and roughness on flotation of glass beads and alumina were studied by measuring the morphological features of particles through different instrumental techniques along with the results of micro-flotation experiments.

1.3 Structure Of The Thesis

This thesis was structured in the form of introduction followed by the papers in Chapter II-V which have been published or submitted during the course of this thesis.

Chapter I presents the main hypothesis, sub-hypothesis, main objective, sub-objectives and scope of this thesis. In Chapter II, the influence of an alternative method namely “Sand Blasting” for producing particles with different morphological properties is

presented. The shape factors of particles were determined with Image Analysis method while the roughness of particles was determined using the Brunauer-Emmett and Teller (B.E.T.) assumption involving the average particle size and real surface area of the particles. In this study, the hydrophobicity of the particles was modified with a commerical collector Flotigam EDA (ethylene-diamine). After determining the optimum concentration with ground particles, flotation studies were carried out at optimum concentration with sand blasted particles. Furthermore, a series of tests were adapted to find out the effect of different blasting parameters such as nozzle pressure, the distance of plate, and the number of blasting on particle morphology, and in turn flotation recovery. It is worth to note that, only the effect of nozzle presure was presented in this study while the optimized values were utilized for other variables. The results of these tests showed the sand-blasting method could well be used for producing particles with different shape factors and roughnesses by changing the nozzle pressure values. Thus, the results of flotation tests carried out with those particles having the same hydrophobicity level suggested that angular and rougher particles yield higher floatation recoveries compared to smooth and round particles (O. Guven, O. Ozdemir, I. E. Karaagaclioglu, M.S. Çelik, 2015, "Surface morphologies and floatability of sand-blasted quartz particles", Minerals Engineering, 70, 1-7). In Chapter III, the influence of abrasion and etching was studied under varying roughness values while maintaining the shape factor of glass bead particles constant. In this study, the roughness of particles was modified with well-known processes as abrasion and acid etching. The hydrophobicity of the methylated particles (TMCS) was determined with contact angle values measured with Drop-Shape Analysis method. Apart from other studies, the degree of roughness of particles was measured with Atomic Force Microscopy. In addition, a theoretical assumption was developed based on a most-cited model (Suresh and Walz model) which is a derivative of DLVO theory with the addition of hydrophobic forces derived from Van Oss theory. Thus, it was found that the calculated energy barrier between rough particles and smooth bubbles decreased even at nano-sized roughnesses of 10-200 nm. From another point of view, the results of flotation kinetics studies also suggested that at higher roughnesses higher flotation rate constants could well be obtained. Interestingly, it was found that any modification on roughness can decrease the energy barrier or in other words enhance flotation rate constant (Onur Guven, Mehmet S. Celik, Jaroslaw W. Drelich, 2015, "Flotation of methylated roughened glass particles and analysis of particle-bubble energy barrier",

Minerals Engineering,79, 125-132). In Chapter IV, the distinction of morphological properties as roughness and roundness values of glass bead particles was presented as a function of their hydrophobicities. In this study, the grinding of glass beads was carried out in a step-wise condition in order to obtain particles with different different morphology. The shape factor analysis indicated that up to a certain grinding time, the shape of particles, spherical in their original form, varied to a definite angularity value above which negligible differences was obtained. In addition, the roughness measurements were performed with optical profilometer where the roughness degree of particles decreased up to certain time which was explained by the simultaneous washing of the particle surfaces during the grinding process. Following the grinding process, abrasion of particles was performed with SiC (Silicon carbide) which is harder than glass beads. It was found that flotation directly correlated with the roundness of particles where it turned out to be the function of roughness obtained in different abrasion times. In short, it was found that shape factors come into prominence at higher hydrophobicities whereas the effect of roughness became pronounced at lower hydrophobicities on flotation recovery values. To our knowledge, this is the first time roughness and shape factor are isolated to distinguish the contribution of each parameter in flotation systems (Onur Guven, Mehmet S. Celik, "Interplay of particle shape and surface roughness to reach maximum flotation efficiencies depending on collector concentration", Mineral Processing and Extactive Metallurgy). In Chapter V, the dependence of flotation on morphology of particles was studied for alumina-SDS system. A similar flowsheet previously applied for the glass bead-amine system was followed. Due to the importance of reagent concentration and pH on alumina-SDS system, all experiments were carried out at optimum conditions which were pre-defined in literature. Therefore, in this study, only the effects of particle morphology in terms of roundness and roughness of particles was studied. The flotation results suggested that higher flotation recoveries could be obtained at lower roundness values for all SDS concentrations studied. In addition, the salient findings for flotation were also confirmed by the high-speed camera recordings which indicated the number of attached particles to the bubbles increased with the increasing roughness values, and in turn increased the flotation recoveries. However, in terms of roughness of the particles, a different trend was obtained which was attributed to the similar hardness of alumina and the abrasive medium used for roughnening their surfaces. Evidently, the difference in flotation recoveries obtained for alumina was not high as that obtained

for the glass beads. However, the effect of variation on shape factor was for the first time investigated for alumina-SDS systems, (Onur Guven, Fırat Karakas, Nurgul Kodrazi, Mehmet S. Celik, “Dependence of morphology on anionic flotation of alumina”, International Journal of Mineral Processing).

2. SURFACE MORPHOLOGIES AND FLOATABILITY OF SAND BLASTED QUARTZ PARTICLES

2.1 Introduction

Sand blasting treatment is an abrasive machining process which is widely used for surface strengthening (Li et al., 1998), modification (Jianxin et al., 2000), cleaning, and rust removal (Djurovic et al., 1999). In this treatment, sand particles are blasted with a shot gun through a nozzle under a certain pressure (bar) in order to change the surface characteristic of the particles.

The behavior of particle systems is primarily affected by the physical characteristics of particles such as size, shape, surface area, roughness, pore size, and structure (Chander et al., 1988; Ulusoy, 1996). In order to describe their physical characteristics, simple linear parameters such as the length, breadth, width, and the ratios of these dimensions can be measured, and used as coefficients to characterize the shape factors in terms of such properties as the aspect ratio, elongation ratio, roundness etc. (Sarkar and Chaudhuri, 1994; Meloy and Williams, 1994; Singh and Ramakrishnan, 1996).

Roughness is another important parameter which is most likely formed due to the fluctuations around a smooth and sharp interface (Szleifer et al., 1986). Almost all surfaces in nature appear smooth for naked eye but they are microscopically rough in various ranges at micro or nano scale. Since the method selected for roughness measurement is important for obtaining reliable data, the morphological characterization of powder sized materials is conducted by two dimensional microscopic measurements from polished sections. However, the main disadvantage of these methods is that the polished sections alter the real morphology of particles (Medelia, 1980). Therefore, three dimensional analyses like BET adsorption by N2 have often been used to obtain reliable data on particle surfaces (Brauner et al., 1938).

[1] This chapter is based on the paper; O. Guven, O. Ozdemir, I.E. Karaagaclioglu, M.S. Celik (2015), "Surface Morphologies and Floatability of Sand-Blasted Quartz Particles, Minerals Engineering, 70, 1-4.

Once the surface area is measured, the roughness of surface can be characterized (Lange et al., 1993). Flotation is a well-known physico-chemical process exploiting differences in surface properties of minerals which depend on wettability or hydrophobicity of particles. Additionally, there are several parameters acting on the efficiency of flotation processes besides other parameters such as collector type, pH, particle size, shape, and other morphological properties of particles. There are several studies on flotation behavior of a liquid partially wetting smooth and rough surfaces (Ulusoy et al., 2005; Yekeler et al., 2003, Rezai et al., 2010). However, in a real world, no surface is totally smooth; hence the status of rough surfaces is still not clear. Moreover, the particle surface roughness with sharp protrusions and edges have a significant effect on film thinning and rupture, which in turn influences the fundamental processes of particle-bubble attachment and other sub processes in flotation (Koh et al., 2009).

In this study, sand blasting equipment was developed and used as a novel approach for producing rough quartz particles at different nozzle pressures. Then, the flotation experiments were carried out with un-blasted and blasted quartz particles in order to investigate the effect of morphology of quartz particles on their flotation behavior.

2.2 Materials and Methods

2.2.1 Materials

The quartz sample used in this study was provided by ESAN mining company, Istanbul, Turkey. The chemical and mineralogical analyses of the sample were carried out by X-Ray Fluorescence (XRF) and X-Ray Diffraction (XRD) methods, respectively. The results presented in Figure 2.1 and Table 2.1, clearly indicate that the sample was pure enough to carry out the experiments.

2.3 Methods

2.3.1 Grinding

The quartz sample was first comminuted by a series of crushers involving jaw, cone, and roll crushers to obtain the particles less than 2 mm in size for the sand blasting experiments. The sample was then ground in a ceramic cylindrical mill. After the grinding, the sample was dry screened using a Ro-Tap sieve shaker for 30 min to obtain

samples of an exact particle size of -0.150+0.075 mm, and this sample was analyzed in terms of shape factor and roughness, and micro-flotation studies.

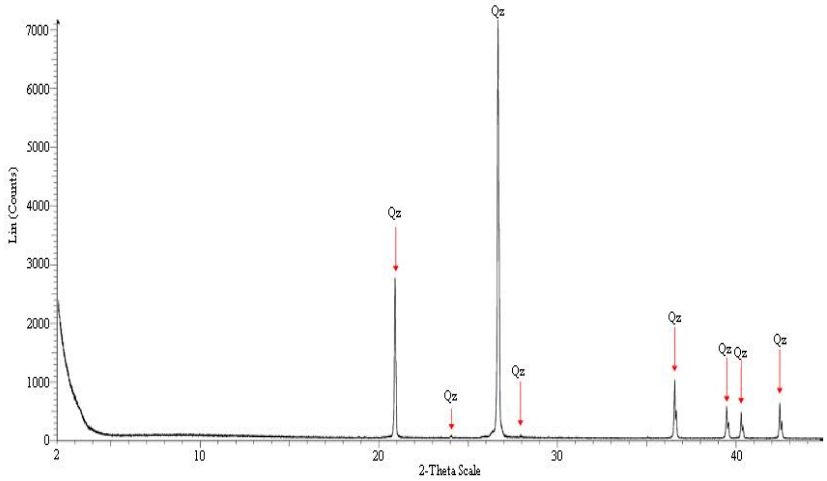

Figure 2.1 : XRD analysis of quartz sample.

Table 2.1 : Chemical analysis of the sample.

Compound	% by weight
SiO_2	98.970
Al_2O_3	0.632
Fe_2O_3	0.095
TiO_2	0.095
MgO	0.096
CaO	0.035
Na_2O	0.034
K_2O	0.043

2.3.2 Sand Blasting

A series of tests were adopted with the uniquely designed sand blasting machine (Figure 2.2) to investigate the effect of blasting on the morphological properties of quartz particles, hence their flotation recoveries. For this purpose, 100 g of crushed quartz sample of less than 2 mm in size was fed to the blasting machine. The quartz particles were blasted with an air stream fan across a high Mn-stainless steel plate where the diameter of nozzle (d) used was 2 cm. The feed speed was kept constant as 0.94 g/s. The air pressure ranged from 1 to 6 bars, and the distance (L) between the plate and nozzle was taken constant as 14 cm.

In this study, a numerical calculation method based on the relation between air pressure (p) and particle velocity (Vp) was used as described in Equation 1.1.

$$V_p \, \alpha \, p^{n_v} \tag{1.1}$$

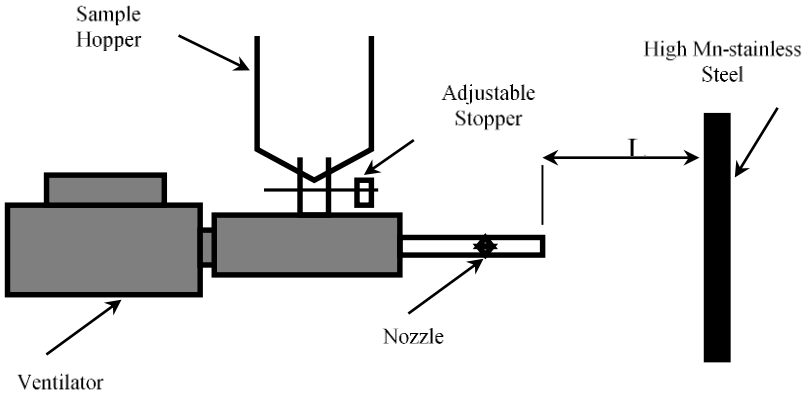

Figure 2.2 : Schematic illustration of the sand blasting equipment and orientation of plate.

Based on the literature data, the power exponent nv was taken as 0.60 (Fokke, 1999) for calculating the particle velocity and plotted against air pressure in Figure 2.3.

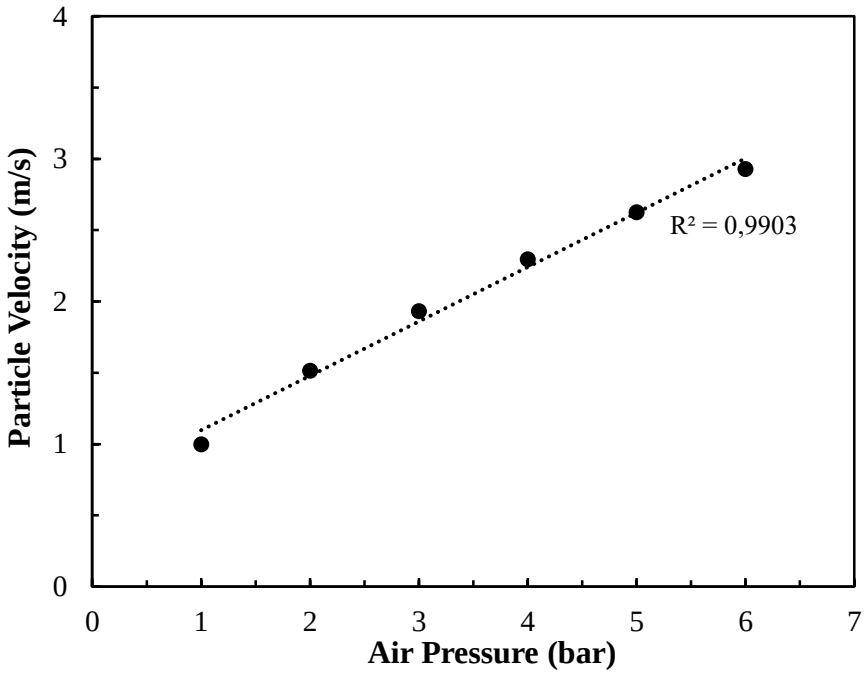

Figure 2.3 : Effect of air pressure on particle velocity.

After the sand blasting, the same screening procedure was applied on the blasted sample to obtain 150×75 μm sized samples. And these samples were also taken for the analysis of the shape factor and roughness, and the micro-flotation studies. The tests were repeated three times in order to obtain reproducible data for evaluating the effect of sand blasting on particle morphology. It is important to note that the same size fraction of 150 × 75 μm was always used in the flotation experiments. Therefore, the

particle size was always kept constant after grinding and blasting processes in order to understand the effect of particle morphology on floatability of quartz.

2.3.3 Sample Characterization

The ground (un-blasted) and blasted samples of 150×75 μm in size were analyzed using QUANTA FEG250 Scanning Electron Microscope (SEM) at magnifications higher than 1500X in order to detect the morphological changes on the particles surfaces.

The image analysis for each representative sample was also performed with Leica QWin Image Analyze Program (Leica QWin User Manual, 1995) based on the particle projections obtained from the photographs. The roundness (Ro), flatness (F), elongation ratio (ER), and relative width (RW) of about 150 particles were automatically calculated by the image analysis software defined as follows (Forssberg et al., 1985):

$$\text{Roundness (Ro)} = \frac{4\pi A}{P^2} \tag{1.2}$$

$$\text{Flatness (F)} = \frac{P^2}{4\pi A} \tag{1.3}$$

$$\text{Elongation Ratio (ER)} = \frac{L}{W} \tag{1.4}$$

$$\text{Relative Width (RW)} = \frac{W}{L} \tag{1.5}$$

Additionally, the surface roughness evaluation based on the specific surface area (area per unit mass or volume) of the un-blasted and blasted quartz particles at different air pressures was determined using QuantachromeTM Autosorp-1 MP device which utilizes the Brunauer-Emmet-Teller (BET) method. In this method, the gas molecules (e.g. N_2) are attracted onto the clean solid surfaces and form adsorbed layers. Under fixed conditions, the extent of adsorption is proportional to the total surface area of the solid (Brunauer et al., 1938). Finally, surface area is calculated from adsorbed gas volume, which is calculated from the difference of pressure and volume of the sample cell. In other words, this method measures the total area which can be reached by the gas molecules used.

Roughness is characterized as the ratio of real surface area to the surface area of a sphere of the equivalent diameter as seen in Equation 1.6.

$$\Lambda = \frac{A_{BET}}{A_{GEOM}} \quad (1.6)$$

In Equation 6, A_{GEOM} represents the geometric surface area which is obtained from the assumption that particles form regular geometric shapes. A_{BET} is the specific surface area calculated using the BET isotherm. Therefore, surface roughness can be calculated from the relationship given in Equation 1.7:

$$\Lambda = \frac{\rho.D.A_{BET}}{6} \quad (1.7)$$

Where, ρ is the density of solid and D is the average particle diameter tested in the equipment. BET equation is easy to apply for most minerals of different structural properties and gives reasonably consistent values for roughness.

2.3.4 Micro-flotation experiments

The micro-flotation tests were carried out with 150×75 μm quartz particles using a 150 cm3 micro-flotation column cell (25×220 mm) with a ceramic frit (pore size of 15 μm) which was mounted on a magnetic stirrer and a magnetic bar used for agitation. A commercial flotation collector namely Flotigam EDA (EDA), an alkyl ether propylene amine with a chemical formula R-O-(CH2)3-NH2, partially neutralized with acetic acid (amine salt) was used.

The flotation tests were carried out with 1 g of both un-blasted and blasted quartz samples. The samples were first conditioned with the collector solutions at desired concentrations for 10 min. In addition, the pH value of the solutions was maintained at pH 9.5 using NaOH. When the conditioning was completed, the suspension was transferred to the flotation cell. Finally, the samples were floated for 1 min using N_2 gas at a flow rate of 60 cm^3/min. The amount of quartz particles in both float and sink products was determined by gravimetric analysis. It is worth to mention that all experiments were repeated three times, and the average flotation recovery value for each test was separately calculated.

2.4 Results and Discussion

2.4.1 Micro-flotation experiments with the un-blasted quartz particles

Many papers have been devoted to the effect of different parameters on quartz flotation. However, the most prominent ones are pH and collector concentration. In this concept, several micro-flotation tests were carried out with the un-blasted quartz particles as a function of EDA concentration at pH 9.5. The reason for selecting this pH is that the solution pH mainly determines the surfactant dissociation or the formation of colloidal amine precipitates in alkaline solutions, hence flotation recoveries can change depending on pH (Laskowski, 1988, Yoon and Yordan, 1990). Therefore, all experiments were carried out at pH 9.5.

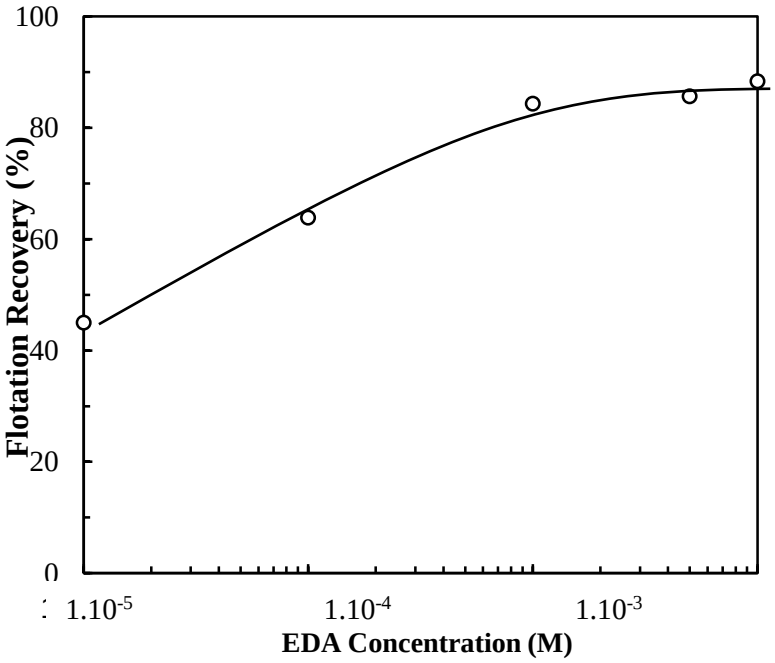

Figure 2.4 : Micro-flotation response of un-blasted quartz particles as a function of EDA concentration.

The flotation results seen in Figure 2.4 showed that the flotation recovery was about 45% at 10^{-5} M collector concentration, and then increased up to 89% at 10^{-3} M, and finally reached the plateau above this concentration. In addition, considering the effect of collector concentration on recovery, our results are consistent with the experimental results reported by Fuerstenau (1957), and Yoon and Yordan (1990).

On the other hand, in this study, an incipient collector concentration at 10^{-5} M EDA was chosen for further flotation tests with the blasted quartz particles in order to

distinguish the effect of sand blasting process along with their morphologies on flotation recoveries.

2.4.2 Micro-flotation experiments with blasted particles

After determining the flotation behavior of the un-blasted quartz particles in terms of collector concentration, a series of micro-flotation tests were performed with the blasted quartz particles as a function of nozzle pressure from 1 to 6 bars in order to show its effect on particle morphologies. Other parameters such as feed speed, and the distance between shot gun and plate were kept constant as 0.94 g/s and 14 cm, respectively. A comparison was also made with the floatability of the un-blasted quartz particles. The micro-flotation test results under the constant conditions are shown in Figure 2.5.

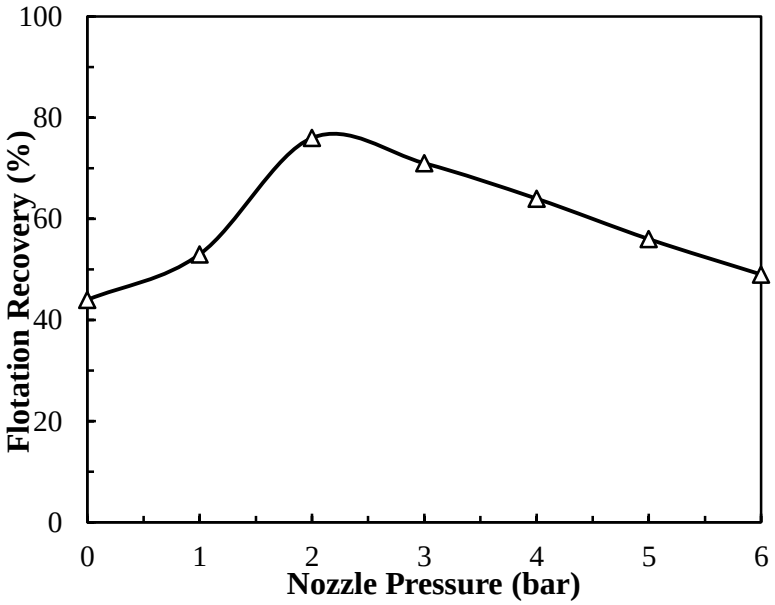

Figure 2.5 : Micro-flotation response of the blasted quartz particles as a function of nozzle pressure.

As seen from Figure 2.5, the recovery of about 40% was obtained with the un-blasted sample. Blasting the sample at 2 bars nozzle pressure increased the recovery up to 80%, and then decreased it gradually down to 50% at 6 bars. These results clearly indicated the significant effect of blasting process induced on the floatability of quartz.

2.4.3 Correlation between particle morphology and flotation recovery

Image Analysis, BET, and SEM techniques were used to analyze the effect of nozzle pressure on the particle morphology of the samples and correlated with the flotation

recoveries. The results are presented in Table 2.2 along with the SEM pictures of the samples given in Figures 2.6 a-f. As seen in Figures 2.6 a-f, the angularity of blasted particles increased compared to the un-blasted particles up to 2 bars of nozzle pressure after that the particles became rounder as a result of hindering of particles during the blasting process. In addition to the angularity, the roughness of the particles also increased up to 2 bars of nozzle pressure, as shown in Table 2.2. However, as can be seen in Figure 2.6 d-f, roughness was also noticed due to "slimes" physically deposited on the particle surfaces. This situation can be explained by the fact that while other parameters such as feed ratio, feed content, and distance between the shot gun and plate were taken constant, only increase in the particle velocity resulted in the blasting of more particles. It also hindered the contact of some particles with the plate or ensured the contact of particular surfaces of the particles; in both cases this implicitly decreased the shape factors of particles produced at un-blasted conditions whereas the flotation recoveries proportionally also decreased.

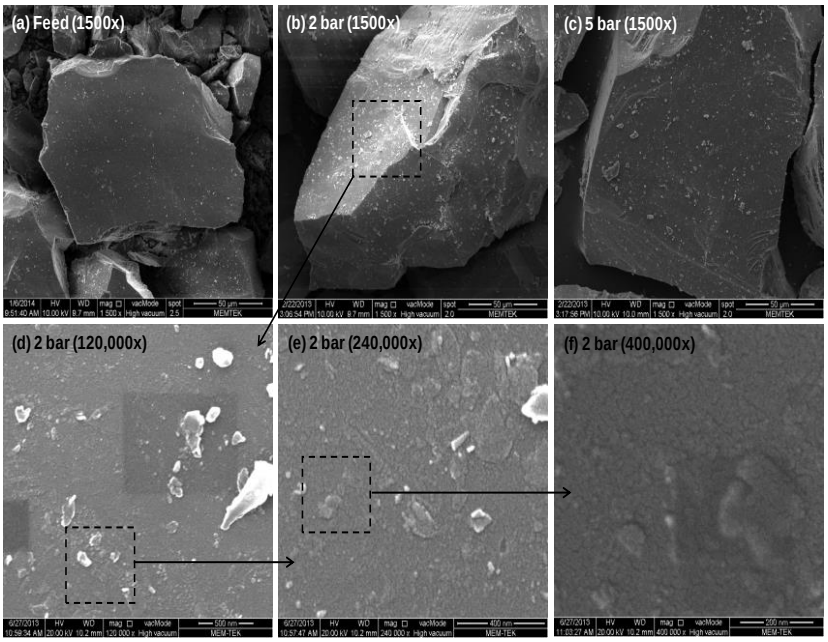

Figure 2.6 : SEM images of the samples (a) un-blasted sample (b) blasted sample at 2 bars (c) blasted sample at 5 bars. (d) Blasted sample at 2 bars (120.000X magnification) (e) blasted sample at 2 bars (240.000X magnification) (f) blasted sample at 2 bars (400.000X magnification).

The results presented in Table 2.2 can also be correlated with the flotation recovery of un-blasted and blasted quartz samples shown in Figure 2.7. As can be clearly seen from Figure 2.7, there is a considerable correlation between the particle morphologies and the flotation recoveries. For example, while the elongation values of the blasted

samples increased with the nozzle pressure up to 2 bars, the flotation recovery concurrently increased. On the other hand, the flotation recovery started decreasing with the increasing the nozzle pressure. This result suggests that the particle surfaces apparently show better floatability at maximum elongations. The results from investigations by Ulusoy et al. 2003, Ulusoy et al., 2005, Ulusoy and Kursun, 2011, Hicyılmaz et al. 2004 on the effect of shape and roughness of particles in flotation also showed that particles possessing higher elongation ratio and flatness properties presented higher recoveries whereas roundness and relative width had a negative effect on the floatability.

Table 2.2 : Shape factors, BET and roughness coefficient of un-blasted and blasted quartz particles.

Nozzle Pressure (bar)	Average Particle Size (µm)	Roundness	Flatness	Relative Width	Elongation	BET Surface Area (m^2/g)	Roughness Coefficient
0	116	0.806	1.241	0.685	1.460	0.22	11
1	119	0.791	1.264	0.678	1.475	0.25	13
2	127	0.786	1.272	0.658	1.520	0.34	19
3	131	0.787	1.271	0.660	1.515	0.29	17
4	122	0.788	1.269	0.675	1.481	0.27	15
5	125	0.800	1.250	0.680	1.471	0.24	13
6	123	0.803	1.245	0.687	1.456	0.24	13

Meanwhile, no measurement of surface tension was made in this study. In addition, these results also imply that the increasing the blasting pressure resulted in more elongated particle surfaces up to 2 bars; such behavior of elongated particles was previously observed by other researchers under different grinding conditions (Ulusoy et al., 2005; Yekeler et al., 2003). Meanwhile, in the literature, the better floatability of elongated quartz particles was attributed to the stronger adhesion force of angular particles which resulted from larger contact areas and longer contact lines compared to the equivalent round particles (Ulusoy et al., 2003; Oliver et al., 1980).

Interestingly, the same trend was also obtained with the particle roughness values seen in Figure 2.8. An increase in nozzle pressure increased the roughness values and also yielded improved flotation recoveries. However, a decrease in the roughness values at increased nozzle pressure hampered the flotation recoveries. These results are also

supported by the SEM pictures of the products presented in Figure 2.6 a-f, i.e., increasing the blasting pressure resulted in more elongated particles and in turn became more angular upon increasing the nozzle pressure. These results could be explained by the fact that increasing the blasting pressure induced different breakage mechanisms resulting in different morphological properties for each particle.

These findings further demonstrated the significance of shape factors involving roundness, flatness, elongation, and relative width with flotation recoveries which is consistent with the literature (Ulusoy et al., 2003; Koh et al., 2009); hence, this can be explained with the better attachment of angular particles to the bubbles (Verelli et al., 2014).

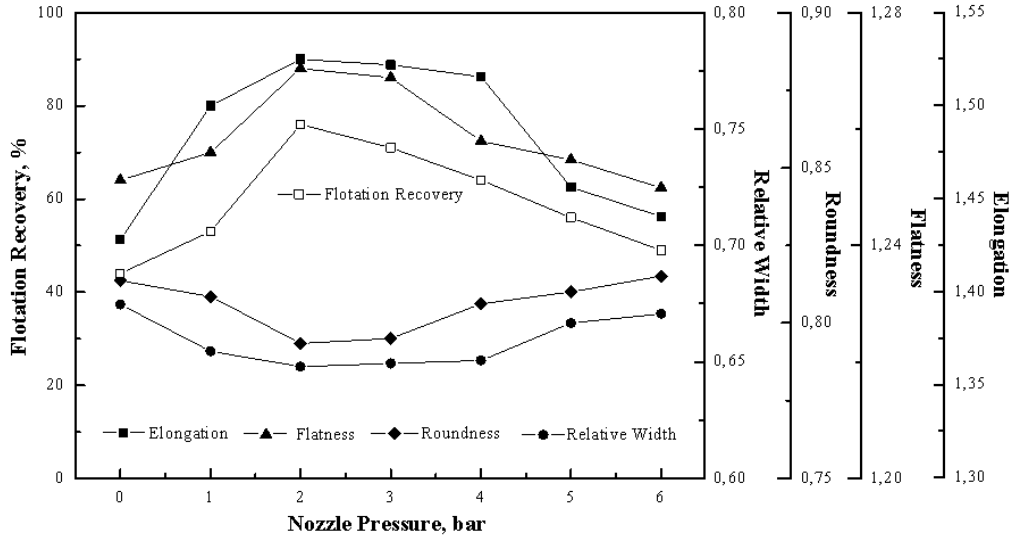

Figure 2.7 : Correlation between shape factors and flotation recoveries for blasted quartz particles produced as a function of nozzle pressure.

The results are consistent with other observations of faster liquids at rough surfaces (Koh et al., 2009; Rezai et al., 2010). In addition, a similar trend was also obtained by Koh et al. for ballotini samples (glass beads used for blasting processes) with different methylation degree and roughness levels where the wettability was reported to decrease with increasing surface roughness and angularity of the particles. However, contrary to these results, some researchers also found that increasing roughness resulted in lower recoveries indicative of higher wettabilities (Ulusoy et al., 2003; Ulusoy and Yekeler, 2004).

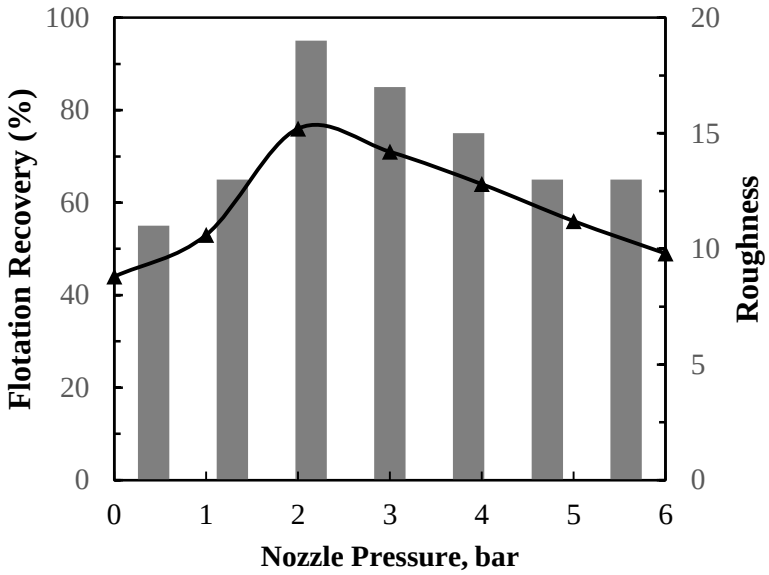

Figure 2.8 : Correlation between flotation recoveries and roughness values of blasted quartz particles produced as a function of nozzle pressure.

In these studies, the researchers investigated the influence of roughness on wettability by correlating their critical surface tension values with average roughness measured by profilometer on pelleted samples, and the degree of wettability was found to be inversely proportional to the critical surface tension (Zisman W.A., 1964). As a result, the materials with lower roughness were found to exhibit lower critical surface tension consequently higher floatability. Similar tendencies for the influence of roughness and shape factors on flotation recoveries were obtained in other studies of the same researchers. However, it is worth to mention that in these studies they used a broad size range of particles (45-250 μm) which could be also significantly influence morphological properties and hence flotation recoveries.

However, recent studies on the correlation of roughness and flotation theory showed that induction time which is the time required for the particle to rupture the bubble was reduced on particles of rougher surfaces (Verelli et al., 2014).

Furthermore, a recent study (Verelli et al., 2014) showed that in the case of angular particles, greater variations could be expected for the induction time measurements. Therefore, the interaction of a particle of an exact geometrical shape (cubic is given as an example) would be the point-first or face-on or other defined interaction types with bubble. Also depending on other parameters such as hydrodynamic resistances, surface chemistry etc., a different induction time mechanism might be expected.

2.5 Conclusions

A new approach was developed for the first time to study the roughness and shape factors of mineral particles produced through a sand blasting machine. Towards this aim, fine quartz particles of 150×75 μm in size were blasted under different nozzle pressures, and the flotation behavior of the blasted quartz particles were compared with the un-blasted particles. The morphology of the particles determined by Image Analysis, SEM methods, and the roughness of the particles inferred by BET method were also correlated with the micro-flotation recoveries. In view of these results, it is clear that roughness has a significant effect on the floatability of particles. A series of systematic tests were conducted to ascertain the effect of different nozzle pressures on both shape and roughness of particles and consequently on flotation recoveries. There appears to be a strong correlation between the shape parameters and roughness values and the flotation recoveries. While floatability of particles increased with increasing flatness and elongation ratios, the surface roughness of particles proportionally increased with the blasting pressure leading to the enhanced floatability of particles. Further research is underway to model the contribution of shape and roughness on adhesion of quartz particles to the bubble.

3. FLOTATION OF METHYLATED ROUGHENED GLASS PARTICLES AND ANALYSIS OF PARTICLE – BUBBLE ENERGY BARRIER

3.1 Introduction

Flotation is a unit operation applied in mineral processing, and sometimes the only process to separate finely grained minerals (Fuerstenau et al. 2007). Particles possessing hydrophobic surfaces, often regulated by the type and amount of collector added to the particles-in-water pulp, are especially susceptible to flotation separation (Albijanic et al. 2014; Ozdemir 2013).

Flotation processes require a wide range of controllable parameters, typically including at least pH, collector type and dosage, and particle size. Recently, there has also been a surge of interest in understanding the influence of morphological characteristics of mineral particles on interactions with bubbles and other particles in flotation pulps (Koh et al. 2009; Verrelli et al. 2014; Verrelli et al. 2011; Ahmed 2010). Particles acquire different morphological characteristics due to the inherent nature of the minerals and as a result of size reduction processes (Verrelli et al. 2014; Holt 1981). From an industrial perspective, the type of grinding process and its conditions have the most important impact on particle morphology (Ulusoy et al. 2004; Ulusoy and Yekeler 2014; Verrelli et al. 2014; Rezai et al. 2010; Ahmed 2010; Koh et al. 2009; Yekeler et al. 2004; Feng and Aldrich 2000). Grinding conditions affect the particle shape—defined through factors such as roundness, flatness, and elongation—and surface roughness (Ahmed 2010). In addition to grinding, the morphological characteristics of particles can be changed through sand blasting technology as presented in recent publications for quartz and glass beads (Guven et al. 2015). The sand blasted particles become more angular and exhibit rougher surfaces at a certain blasting pressures, and these particles reported to froth ahead of less rough particles.

[2] This chapter is based on the paper; Onur Guven, Mehmet S. Celik, Jaroslaw Drelich, "Floatability of roughened methylated glass bead particles and analysis of particle-bubble energy barrier, (2015), 79, 125-132.

As early as in 1977, Anfruns and Kitchener (Anfruns and Kitchener 1977) suggested that surface asperities stimulate rupture of the intervening aqueous film during particle-bubble attachment, resulting in enhanced flotation of particles. Then Ducker et al. (Ducker et al. 1989) demonstrated improved flotation of ground quartz over ballotini glass spheres in the presence of an amine collector. More recently, Feng and Aldrich (Feng and Aldrich 2000) investigated the effect of milling conditions on the flotation kinetics of complex sulfide ores. They found greater flotation rate constants for dry ground particles than wet ground ones and attributed it to differences in surface roughness characteristics with rougher particles produced during dry milling. Similar findings reported by Rezai et al. (Rezai et al. 2010) stressed that an increase in flotation rate constants was proportional to the roughness characteristics. Yekeler et al. (Yekeler et al. 2004) observed that rougher talc particles reporting to the concentrate were less smooth than those collected in the tailings. All these findings indicate a positive effect of surface roughness on flotation of hydrophobic particles in electrolyte solutions. There is, however, no understanding why roughness of particles is so important in flotation.

Flotation of mineral particles is controlled by particle trajectories in complex suspensions made of an aqueous solution, mineral particles and gas bubbles, and bubble – particle colloidal interactions (Ralston et al. 2002). Trajectories of movement of rough and irregular particles can be different than for spherical ones, which could trigger differences in probabilities for collisions of particles with gas bubbles (Verrelli et al. 2014; Schmidt and Berg 1996). However, as it will be demonstrated in this contribution, the flotation recovery and kinetics are still different in carefully designed flotation experiments involving spherical particles having only dissimilarity in a sub-microscopic roughness. In these experiments any differences in hydrodynamic conditions are minimal, if present at all. To explain the effect of particle roughness on flotation rate and recoveries, colloidal forces operating between particles and gas bubbles will be analyzed theoretically using the extended – DLVO model. Despite the multitude of publications on modeling of colloidal interactions in systems with spherical particles or flat surfaces, only a few investigators have focused on the colloidal interactions involving rough surfaces (Bhattacharjee et al. 1998; Hoek et al. 2003; Suresh and Walz 1996, 1997; Walz et al. 1999; Sun and Walz 2001; Hoek and Agarwal 2006). None of them however, analyzed the particle – bubble energetic

barrier, which controls the particle-to-bubble attachment process in flotation of minerals (Laskowski et al. 1991).

3.2 Experimental

3.2.1 Glass particles and their preparation

The glass particles used in this study were standard safety glass spheres with the size of 150 ×106 μm and supplied by Potters Industries. The elemental analysis performed by the X-ray fluorescence (XRF) technique revealed the glass to be composed of 61.3 wt% of Si, 14.8 wt% Ca, 13.1 wt% Na, 6.0 wt% Al, 3.8 wt% Mg, and 1.0 wt% Fe.

The roughness of glass particles was changed through either abrading or acid etching. About 50 g of glass particles were dry abraded in a laboratory drum with 1 μm Dupont brand abrasive alumina (Al_2O_3) powder for 3 hours. The reason for using such fine material was to avoid any size reduction of glass beads during the abrasion process. The abraded glass particles were wet screened through 106 μm sieve, water washed several times, dried, and stored in glass bottles.

Another 50 g of glass particles were etched with hydrofluoric acid solution following a procedure presented in the literature (Dang-Vu et al., 2006). Glass particles were dipped into 10 v/v % HF solution for 5 min followed by dipping in etching solution for 10 min. The etching solution consisted of distilled water (35 v/v %), 49 v/v % HF acid (30 v/v %), and KHF_2 (35 v/v %). They were then dipped into HF acid solution for another 3 min. The modified glass particles were washed with distilled water and dried over night at 110 ºC.

All particles were washed multiple times to remove any organic and inorganic contaminants remaining on the surfaces of original and roughened glass particles. The particles were treated with acidic (2.5 v/v % H_2SO_4) and then basic (2.5 w/v % NaOH) solutions, and next washed with distilled water. Then the samples were suspended to 20 wt. % with tap water in a glass bottle and rolled gently at 150 rpm for 24 h. The slurry was subsequently filtered and dried at 110 ºC in an oven overnight. The dried particles were then washed with: a) Micro-90 detergent solution; b) deionized water until all detergent was removed; c) boiled in H_2O:H_2O_2:NH_3 (5:1:1 v/v) mixture; d) washed with deionized water; e) washed with absolute ethanol; and finally dried in oven at 110ºC.

Analytical grade trimethylchlorosilane (TMCS) from Aldrich and cyclohexane (as solvent) obtained from Fisher Chemicals were used for the methylation of glass particle surfaces. These chemicals were used as received without further purification. Glass particles, with smooth and rough surfaces, were methylated to enhance their hydrophobicity and affinity for air bubbles in electrolyte solutions. The method used is similar to that reported in the literature (Koh et al. 2009). The methylation was carried out with 10 g batches of glass particles and involved contacting excess amounts of diluted TMCS in cyclohexane in a reaction vessel overnight to induce the following reaction: $\text{-Si-OH+(CH}_3)_3\ \text{SiCl}\rightarrow\text{-Si-O-Si(CH}_3)_3\text{+HCl}$. The concentration of TMCS in the reaction vessel was calculated based on the molecular weight of TMCS (108.64 g/mol), by diluting it with cyclohexane. TMCS concentrations varied from 0.00001 M to 0.01 M to explore a wide range of hydrophobicity of glass particles. After completion of the methylation, the samples were washed with solvent, air-dried, and stored in a desiccator.

3.2.2 Imaging of particles

Glass particles were imaged with a JEOL JSM-6400 scanning electron microscope (JEOL USA, Inc, Peabody, MA) using 20 kV accelerating voltage. To enhance conductivity, the particles were attached to aluminium mounts with double – sticky carbon – based conductive tape and coated with a gold/palladium alloy to 5 nm thickness. Digital images (512 x 512 pixels) were acquired with dPict7 software (Geller Micro Analytical, Topsfiled, MA)

A Nanoscope III Dimension 3000 atomic force microscope (Digital Instruments, Santa Barbara, CA, USA) was used in a Tapping mode operation for topographical imaging of individual glass particles and determination of their surface roughness. Budget Sensors Tap300Al cantilevers made of silicon with an aluminum reflex coating, and an estimated tip radius of 10 nm – as per manufacturer's specification – were used in this study. The particles were mounted on glass slides through double – sticky adhesive tape. Roughness characterization included root-mean-square (RMS; also often called geometrical roughness (Rq)) that represents a measure of the standard height deviation for the analyzed image area, and the arithmetic average of the absolute values of surface height deviations from the mean (Ra).

3.2.3 Hydrophobicity of particles

The success of glass methylation via quantification of surface hydrophobicity was determined through advancing contact angle measurements for deionized water. Due to technical challenges associated with direct measurement of contact angles on 106 – 150 μm particles, 2 mm particles made of the same borosilicate glass and supplied by the same vendor were used instead. The methylation of 2 mm particles was carried out in the same solutions and under the same conditions, including washing and drying, as described earlier for 106 – 150 μm particles.

The contact angle measuring technique used here was a sessile – drop method adapted to a curved surface. In this study only advancing (static) contact angles were measured. A water droplet having a ~1 – 2 μl volume was placed over the apex of 2 mm glass particles. The image of one of the particle with deposited water droplet is shown in Figure 3.1a. This figure also shows the primary parameters and dimensions important to measurements of contact angles. Two equations describing the geometry, from which contact angle (θ) was calculated, are:

$$tan\left(\frac{\theta+\alpha}{2}\right) = \frac{2h}{d} \tag{3.1}$$

$$d = D \sin \alpha \tag{3.2}$$

where h is the height of the deposited water droplet, d is the diameter of droplet base, D is the diameter of droplet.

The images of at least 6 droplets were captured by Krüss G10 Contact Angle Measurement System within 15-30 s after their deposition. The multiple measurements allowed to calculate the mean values and standard deviations reported in Figure 3.1b.

3.2.4 Micro-flotation separation tests

Micro-flotation tests were carried out in a homemade 150 cm^3 micro-flotation column cell (25x220 mm) with a ceramic frit having a pore size of 15 μm, mounted over a magnetic stirrer; a magnetic bar was used for agitation. 1 g of glass particles were conditioned in 0.001 M NaCl for 5 min before injection of gas. Either particles of the same surface roughness characteristics or a mixture of two different ones were used in the experiments. Throughout all micro-flotation tests 10 ppm MIBC (methyl isobutyl carbinol) frother was used. High purity nitrogen was used to maintain gas flow rate of

about 45 cm^3/min throughout the entire flotation experiment. The floated particles were collected at 20, 40, 60, and 80 seconds intervals, washed, dried and then weighed.

In this study, the classical first-order rate model was applied to evaluate the flotation kinetics:

$$R = R_\infty(1 - e^{-kt}) \tag{3.3}$$

where R is the recovery at time t, R_∞ is the ultimate recovery, k is the first order rate constant (min^{-1}).

3.3 Results and discussion

3.3.1 Surface characteristics of particles

Figure 3.2a shows SEM micrographs for untreated particles, followed by micrographs of particles roughened through milling and acid etching. A few micrometer sections of surfaces were also imaged with the AFM and selected images are shown in Figure 3.2b. Both SEM micrographs and 3- dimensional AFM surface profiles clearly indicate differences in surface roughness characteristics among three batches of particles used in this study. As expected, the untreated particles were the least rough, with RMS and Ra values of varying only from ~1 to 10 nm and ~1 to 8 nm, respectively. A spread in these values reflects surface texture variation among different particles and different surface segments for the same particle. The RMS and Ra roughness values however, clearly indicate that the glass particle surfaces were nearly smooth.

Milling of the glass particles with alumina powder increased roughness to RMS = 10 – 30 nm and R_a = 6 – 18 nm. Although both RMS and Ra increased a few times, the roughness remained at a level of several nanometers in most of the surface segments. The milling produced relatively uniform roughness characteristics and importantly, did not affect the particle shape and size.

On the contrary, more localized roughness, reflected in symmetrical bowl-shaped valleys, was produced during the acid etching (Figure 3.2a). The etching solutions and duration were carefully selected and strictly controlled to preserve the size and spherical shape of particles. The particle surface analysis with AFM instrument revealed that the roughness produced was still sub-microscopic with RMS = 34 – 270 nm and R_a = 28 – 170 nm values. A broader variation in roughness values is

understandable here, and reflects localized etching features randomly distributed through particle surface.

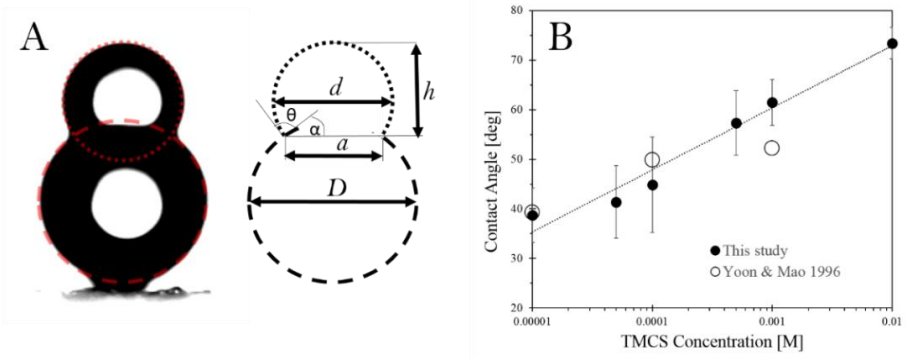

Figure 3.1 : (a)Image of a water droplet on top of 2 mm glass sphere and schematic of the system with all major geometrical parameter used in calculations of contact angles; (b) the water contact angle values measured for glass particles metyhlated in cyclohexane solutions of trimethylchlorosilane (TMCS) of varyinh molar concentration. The bars represent standard deviation at 95% confidence level. The literature values were taken from publication by Yoon and Mao and were obtained for glass slides methylated with TMCS using similar conditions (Yoon and Mao, 1996).

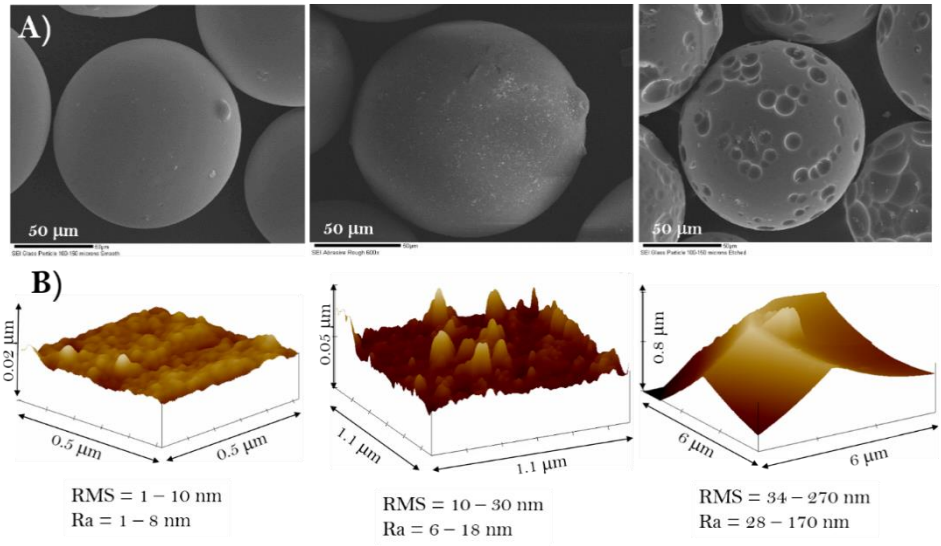

Figure 3.2 : (a) SEM micrographs of glass particles; and (b) AFM images of small sections for these particles with RMS and R_a roughness values recorded from multiple images.

Figure 3.1b summarizes the advancing contact angles (θ_A) measured for water droplets on 2 mm glass particles, surfaces of which were hydrophobized with TMCS solutions of varying concentration. The contact angle values increased from about 39 to 73 degrees when methylation was carried out with 10^{-5} to 10^{-2} M TMCS solutions. The contact angles obtained on curved surfaces in this study are nearly identical to those reported for glass slides methylated under similar conditions (Yoon and Mao 1996).

Relatively large scatter of the measured contact angle values reflected in standard deviation for the mean value, which varied from 3 to 10 degrees, is the result of two effects. First, placing the water droplet exactly over the apex of a 2 mm particle is a challenge and a small departure for the needle axis from alignment with the axis of particle apex can cause asymmetrical spread and deposition of the water droplet. Second, even a small gradient in hydrophobicity or roughness around particle apex could shift the symmetry of the water droplet. A variation in the distribution of adsorbed TMCS molecules that resulted in more heterogeneous nature of the particle surface was quite evident from the characteristic corrugation of water droplet base, and was particularly evident at lower surface coverages of trimethylchlorosilane. Any asymmetry in the profile of the deposited water droplet made the measurements of droplet dimensions less accurate.

Only particles methylated in 10^{-5} M (θ_A = 39 + 5 degrees) and 10^{-2} M (θ_A = 73 + 3 degrees) TMCS solutions were used in flotation experiments described in the next sub-section.

3.3.2 Micro flotation test results

Figure 3.3 presents flotation results for 106 - 150 μm glass particles of varying surface characteristics (smooth, abraded and acid etched) which were methylated in either 10^{-5} M or 10^{-2} M TMCS solutions. All the tests were carried out at natural pH and constant ionic strength of 10^{-3} M NaCl concentration. As expected, more hydrophobic methylated glass particles with water contact angle of about 73 degrees floated at higher recoveries and rates than particles with water contact angle of about 39 degrees.

The linear correlations between ln (100-R) and time in Figure 3.3a,b validate the first order kinetics for flotation of methylated glass particles, equation (3). The calculated flotation rate constant (k) values are shown in Figure 3.3c. The flotation rate constant for untreated particles (with the smoothest surfaces) that was hydrophobized in 10^{-5} M TMCS solution was only 0.1 min^{-1}. Roughening of the glass particle surfaces enhanced their floatability. The flotation rate constant doubled after abrading their surfaces with alumina powder, and tripled after acid etching (Figure 3.3c). When larger fraction of particle surfaces was covered with trimethylchlorosilane, the particles floated at a rate almost one order of magnitude greater.

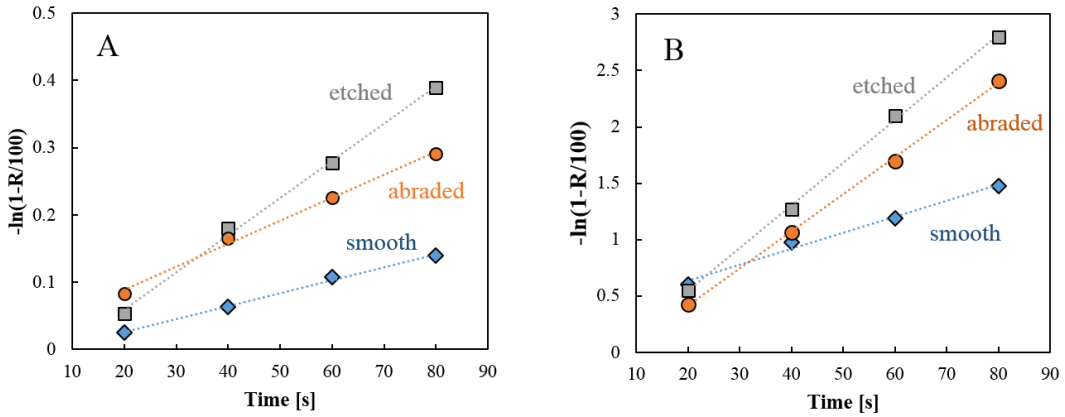

C

Particles	Rate constant, k [min^{-1}]	
	$\theta_A = 39 \pm 5^o$	$\theta_A = 73 \pm 3^o$
Smooth	0.1	0.9
Abraded	0.2	2.0
Acid etched	0.3	2.3

Figure 3.3 : Flotation kinetics of glass particles methylated in (a) 10^{-5} M (θ_A = 39±5 degrees), (b) 10^{-2} M (θ_A = 73±3 degrees) TMCS solutions, and (c) calculated flotation rate constants.

Also, the flotation rate was smallest for untreated particles, followed by abraded and then acid etched particles. In other words, the flotation separation increased with increasing particle surface roughness and hydrophobicity.

We also found that rough particles preferentially floated from a 1:1 mixture of smooth and rough particles (either abraded or acid etched). After 80 seconds of flotation, the scanning electron microscopy imaging (not shown) revealed that particles in tailings comprised mostly of particles with smooth surfaces and only ~17 to 22 % of particles had rough surfaces.

Our results on enhanced flotation of rough particles are in agreement with the results of previous studies. For example, Ducker et al.(Ducker et al. 1989) demonstrated improved flotation of ground quartz over ballotini glass spheres in the presence of an amine collector. They attributed the enhanced flotation to a reduction of the area of interactions and consequently reduced repulsions faced by rough particles approaching gas bubbles. A similar effect was recently reported for glass particles methylated under conditions similar to those used in our study (Verrelli et al. 2014). Verelli et al. examined the flotation kinetics of both smooth and ground glass particles as a function of methylation degree. They found that, under the same methylation conditions and flotation time, the ground particles floated easier than the smooth ones and as a result, the flotation rates were higher for ground particles. This effect was attributed to

accelerated thinning and rupturing of the thin aqueous film at a rough particle surface. Indeed, the time for a gas bubble attachment to the solid surface is typically reduced by the surface roughness. For example, a gradual decrease in bubble attachment time from 80 to 2-3 ms was reported for the Teflon plates of increasing roughness (Krasowska and Malysa 2007). Also, attachment times are typically one to two orders of magnitude shorter for bubbles on flat substrates compared to bubbles pressed into a bed of ground (irregular and rough) particles (Drelich and Miller 2012). Since bubble attachment or induction time is related to flotation kinetics and resulting recoveries, the particle surface roughness appears to foster the flotation process.

Beside enhanced flotation, we also observed in our experiments that rough particles agglomerated to a larger extent and their dispersion in the electrolyte solution was more difficult than for particles with smooth surfaces.

3.3.3 Energy barrier analysis

Stability of an aqueous film and associated energy barrier that prevents the particle from attachment with the surface of a gas bubble can dictate the outcome and rate of flotation processes (Laskowski et al. 1991). Little attention was given however, to understanding and quantification of energy barrier in particle – bubble interactions. Here, we demonstrate theoretically that the energy barrier between methylated glass particles and the surface of air bubbles can be of a significant magnitude. More importantly, we show that surface sub-microscopic roughness can reduce the energy barrier value by orders of magnitude and most likely could explain better flotation performance of methylated glass particles with roughened surfaces as compared to smooth ones.

Retarded van der Waals, electrical double layer, and hydrophobic interactions were included in our theoretical analysis for rough particle – electrolyte solution – bubble surface system allowing quantify the energy barrier associated with these three interactions. Energy of interactions that combine both retarded van der Waals and electrical double layer contributions (known as DLVO interactions) were calculated according to the model derived earlier (Suresh and Walz 1996). Here we also added the Lewis acid – base interaction model (van Oss 1994) that provides quantification of hydrophobic effects, after it was modified to reflect the rough particle – surface geometry. Although a few different equations were proposed in the literature to

describe hydrophobic interactions, the Lewis acid – base interaction model was selected in this study due to our previous success in using it to describe interactions for hydrophobic coal particles in high ionic strength solutions (Nguyen et al. 2007).

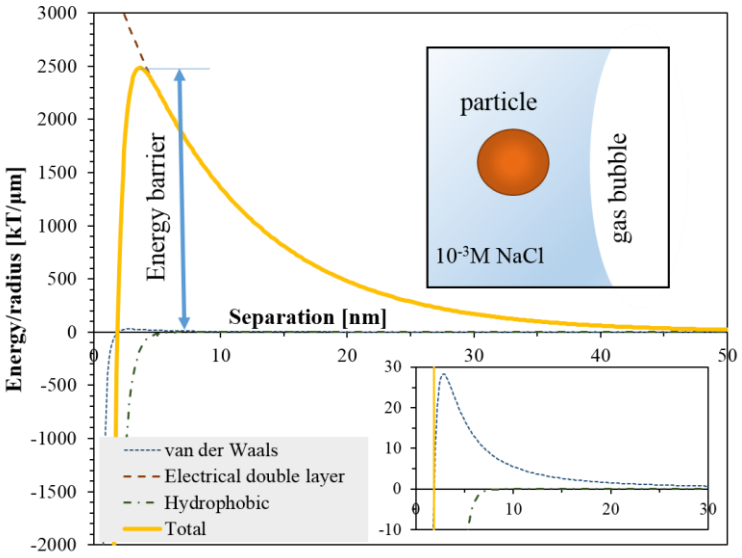

Figure 3.4 : Interaction energy between 100 μm methylated glass particle and flat surface of gas bubble normalized per radius of the particle. The total energy is the result of van der Waals, electrical double layer and hydrophobic interactions. The following parameters were used: (i) for van der Waals interactions (A=-5.47x10^{-21} J, λ = 40 nm); (ii) for electrical double layer interactions (ψ_1 = - 33 mV, ψ_2 = - 63 mV, κ^{-1} = 9.6 nm); and (iii) for hydrophobic interactions (λ_{AB}=0.6 nm, h_0=0.157 nm and ΔG_0= - 60 mJ/m^2). Insert at the lower right corner shows van der Waals and hydrophobic energy at separations below 30 nm.

Also, Hoek and Agarwal (Hoek and Agarwal 2006) demonstrated that Lewis acid – base interactions can control interactions between nano-sized particles and rough substrates. All equations used in our calculations are listed in the Appendix.

Figure 3.4 shows the changes in total, retarded van der Waals, electrical double layer, and hydrophobic interaction potentials for varying separations between a spherical particle and a surface. The Hamaker constant of A = -5.47 x 10^{-21} J for the methylated glass – water – air bubble system was taken from Yoon and Mao (Yoon and Mao 1996). Other parameters for retarded van der Waals interactions were adopted from Suresh and Walz (Suresh and Walz 1996). Surface potential for a gas bubble (ψ_1 = - 33 mV) and methylated glass particle (ψ_2 = - 63 mV) were adopted from Yoon and Mao (Yoon and Mao 1996). Here the deformability of bubble surface is neglected to simplify the analysis of colloidal interactions. The selected Debye length of κ-1 = 9.6 nm reflects the 0.001M NaCl solution used in flotation experiments. Parameters for

hydrophobic forces (λ_{AB} = 0.6 nm, h_0=0.157 nm, ΔG_0= - 60 mJ/m^2) were arbitrarily selected after van Oss (van Oss 1994) to reflect weakly hydrophobic particles, typical to mineral flotation.

Figure 3.5a,b shows the effect of asperities and their size on spherical particle – bubble surface interactions and resulting decrease in energy barrier. These effects are consequences of nano – sized hydrophobic asperities penetrating the aqueous film that separates the rough particle from the surface (representing a gas bubble surface). It is quite obvious from the model used in this study that if the particle – surface gap (h) becomes larger than the asperity size (εs) the extent of roughness effect and thus the interaction between rough and smooth surfaces becomes relatively insignificant (Figure 3.5a).

As shown in Figure 3.5a, adding hydrophobic asperities with a radius of ε_S = 10 nm reduces the energy barrier value for particle – surface interactions nearly by half. Increasing the size of asperities from ε_S = 10 to ε_S = 70 nm lowers the energy barrier value by two orders of magnitude and pushes it to larger separation distances. The correlation between the energy barrier value and the asperity size is shown in Figure 3.5b. Reduction in energy barrier value shown in Figure 3.5b is the direct result of hydrophobicity of asperities. A shift in location of maximum interaction potential value to larger separation values is controlled by particle – surface electrostatic repulsions.

The above theoretical findings suggest that asperities of rough particles at a level of only a few nanometers should have a pronounced impact on the probability of particle attachment to gas bubbles, since overcoming a smaller energy barrier should be easier. In fact, any nanoscopic roughness of hydrophobic particle surfaces should enhance flotation; the same should be true regarding coagulation of particles. These findings, in our opinion, indirectly explain the results of micro-flotation discussed in the previous sub-section since the majority of asperities for glass particles used was with dimensions of ~10 nm for abraded particles and 40-100 nm for acid etched particles. It also agrees with previous suggestions on effects of pretruding asperities of rough surfaces on surface forces in dispersed systems (Ducker et al. 1989) and stability of aqueous film separating particles from plates (Anfruns and Kitchener 1977).

The findings of this research further suggests that designing of crushing and grinding operations that could produce rough particles with sub-microscopic asperities could lead to improvements in flotation separation. This is in addition to previous findings which demonstrated a positive effect of ionic strength in depressing the energetic barrier between hydrophobic coal particles and gas bubbles, important criterion in enhanced flotation of coals (Nguyen et al. 2007; Pineres and Barraza 2011).

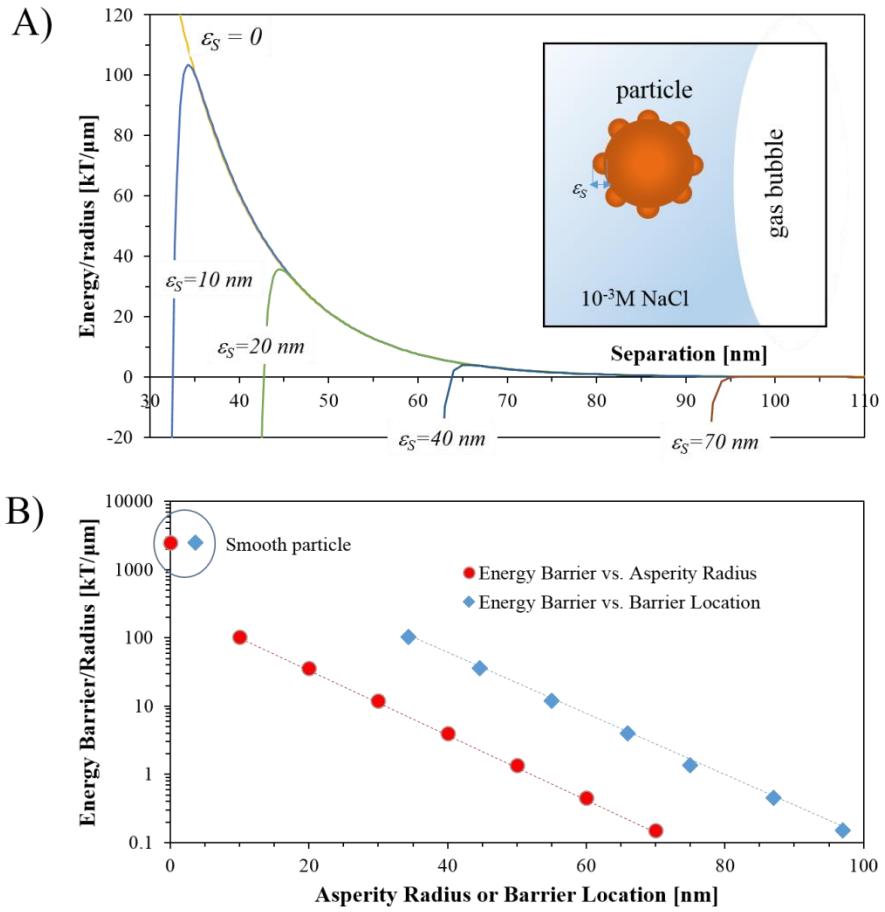

Figure 3.5 : The effect of asperity height values on total energy profiles for the particle-bubble interaction.The particle surface coverage by nanoasperities was θ = 0.001. Other parameters included:I) for van der Waals interactions (A = -5.47x10^{-20} J, λ = 40 nm); ii) for all double layer interactions (ψ_1 = -33 mV, ψ_2 = -63 mV, κ^{-1} = 9.6 nm); and iii)for hydrophobic interactions (λ_{AB} = 0.6 nm, h_0=0.157 nm, ΔG_0= - 60 mJ/m^2).

3.4 Conclusions

In this study, 150x106 μm spherical glass particles were abraded with fine alumina powder and acid etched to produce particles of nano – scaled surface roughness characteristics. The roughening protocol preserved sphericity of the glass particles.

Untreated and roughened glass particles were cleaned and methylated, and then underwent micro – flotation separation from 0.001M NaCl solution. The flotation results confirmed a positive effect of particle surface roughness on their flotation kinetics and recoveries. The flotation rate constant for methylated glass particles, with hydrophobicity defined by the water contact angle of ~39 degrees was determined to be 0.1 min-1, and this value doubled and tripled for abraded and acid etched particles of the same hydrophobicity, respectively. The flotation rate constants increased to 0.9, 2.0, and 2.3 min-1 for the same particles, respectively, after hydrophobicity of the glass particles in terms of water contact angle increased to ~73 degrees.

To explain differences in flotation of spherical particles with smooth and rough surfaces, a theoretical model on DLVO interaction energy for particles decorated with hemispherical nano–asperities and flat surfaces was adopted to this research. Lewis acid – base interaction energy was also incorporated to this model to reflect hydrophobic attractive interactions typical to flotation systems. It was found that hydrophobic asperities with radius as small as 10 – 70 nm can reduce the energy barrier against particle attachment to a gas bubble by one to two orders of magnitude.

3.5 Appendix – Theoretical Model

Modeling of rough particle – flat surface interaction energy included retarded van der Waals (E_{vdW}), electrical double layer (E_{EDL}) and hydrophobic interactions (E_H). The model of the particle covered with hemispherical asperities of radius ϵ_S, their surface density n and coverage θ was adopted from the literature (Suresh and Walz 1996). Also equations describing the DLVO energies derived for rough particle – flat plate geometry were directly adopted from the same reference.

The equation describing the retarded van der Waals interaction potential between a particle and flat surface is as follows (Suresh and Walz 1996): for rough spherical particle – flat surface geometry,

$$E_{vdW-RS} = 2\pi RA\left[\frac{-2.45\lambda}{120\pi^2 h^2} + \frac{2.17\lambda^2}{720\pi^3 h^3} - \frac{0.59\lambda^3}{3360\pi^4 h^4}\right] + n\pi\left(\frac{2.45\lambda AR}{30\pi}\right)\left[\frac{\epsilon_S{}^2}{2h^2} + \ln\left(\frac{h}{h-\epsilon_S}\right) - \frac{\epsilon_S}{h-\epsilon_S}\right] - n\pi\left(\frac{2.17\lambda^2 AR}{360\pi^2}\right)\left[\epsilon_S{}^2\left(\frac{1}{h^3} - \frac{1}{(h-\epsilon_S)^3}\right) - \frac{1}{h} + \frac{1}{h-\epsilon_S} - \frac{\epsilon_S}{(h-\epsilon_S)^2} + \frac{\epsilon_S{}^2}{(h-\epsilon_S)^3}\right] + n\pi\left(\frac{0.59\lambda^3 AR}{840\pi^3}\right)\left[\epsilon_S{}^2\left(\frac{1}{2h^4} - \frac{1}{2(h-\epsilon_S)^4}\right) - \frac{1}{6h^2} + \frac{1}{6(h-\epsilon_S)^2} - \frac{\epsilon_S}{3(h-\epsilon_S)^3} + \frac{\epsilon_S{}^2}{2(h-\epsilon_S)^4}\right] \quad (3.4)$$

which reduces for smooth spherical particle – flat surface geometry to the following,

$$E_{vdW-SS} = 2\pi RA\left[\frac{-2.45\lambda}{120\pi^2h^2} + \frac{2.17\lambda^2}{720\pi^3h^3} - \frac{0.59\lambda^3}{3360\pi^4h^4}\right] \quad (3.5)$$

where A is the Hamaker constant, R is the radius of the spherical particle, λ is the characteristic wavelength, n is the number density of asperities ($n = \theta\pi\varepsilon_s^2$) and θ is their surface coverage, ε_s is the asperity height (radius), h is the separation distance as measured from the sphere surface.

Equations describing the electrical double layer interaction potential between a rough sphere and a plate are (Suresh and Walz 1996), for rough spherical particle – flat surface geometry,

$$E_{EDL-RS} = 16R(4\pi\epsilon\epsilon_0)\left(\frac{kT}{e}\right)^2 \tanh\left(\frac{e\psi_1}{4kT}\right)\tanh\left(\frac{e\psi_2}{4kT}\right)(1 - n\pi\epsilon_S{}^2)e^{-\kappa h} + \frac{8n\pi\epsilon_S}{\kappa}R(4\pi\epsilon\epsilon_0)\left(\frac{kT}{e}\right)^2 \tanh\left(\frac{e\psi_1}{4kT}\right)Y_3 e^{-\kappa(h-\epsilon_S)} \quad (3.6)$$

which for smooth spherical particle – flat surface geometry becomes,

$$E_{EDL-SS} = 16R(4\pi\epsilon\epsilon_0)\left(\frac{kT}{e}\right)^2 \tanh\left(\frac{e\psi_1}{4kT}\right)\tanh\left(\frac{e\psi_2}{4kT}\right)e^{-\kappa h} \quad (3.7)$$

where ψ_1 and ψ_2 are the surface potentials of gas bubble and methylated glass particle, respectively, k is the Boltzmann constant (1.38x10-23 m^2 kg $s^{-2}K^{-1}$), e is the charge of a proton (1.602x10^{-19} C), T is the temperature (298 K), κ^{-1} is the Debye length, ε is the bulk dielectric constant (80), ε_0 is the permittivity of free space (8.85x10^{-12} $C^2J^{-1}m^{-1}$) and Y_3 is the effective surface potential of the asperities on the rough particle surface-defined by Bell et al. (Bell et al. 1970) as $Y_3 \cong 4\tanh((e\psi_3)/4kT)$ – in the case considered in this study, $\psi_3 = \psi_2$ (Walz et al. 1999). For calculation of hydrophobic interaction potential the Lewis acid – base model was adopted (van Oss 1994). Since no analytical solution to Lewis acid – base interactions was provided in the past for the rough particle – flat plate geometry considered in this study, a set of equations was derived starting with the interaction potential for two infinite plates (van Oss 1994):

$$E_H = \Delta G_0 \exp\left(\frac{h_0 - h}{\lambda_{AB}}\right) \quad (3.8)$$

where λ_{AB} (=0.6 nm) is the decay length for acid-base interactions in water, h_0 (=0.157 nm) is the minimum separation distance due to the Born repulsion, and ΔG_0 is the free energy of acid-base interactions defined as $\Delta G_0 = 2(\sqrt{\gamma_s^-\gamma_l^+} + \sqrt{\gamma_s^+\gamma_l^-}) - 4\sqrt{\gamma_l^-\gamma_l^+}$. In order to calculate the interaction potential between a rough particle and a smooth surface the Derjaguin approximation (Derjaguin 1934) was used:

$$E_{H-RPS} = 2\pi R\int_h^\infty E_{H-RS}\, dh \quad (3.9)$$

Here the expression on the interaction potential for hydrophobic interactions ($E_{H\text{-}RS}$) operating between the rough surface and the smooth surface (R) is defined as:

$$E_{H-R} = E_H(1-\theta) + nE_{H-A} \tag{3.10}$$

with $E_{H\text{-}A}$ as the interaction potential between a hemispherical asperity and smooth surface that is equal to:

$$E_{H-A} = 2\pi\varepsilon_S \int_{h-\varepsilon_S}^{\infty} E_H \, d(h-\varepsilon_S) \tag{3.11}$$

As the result of integrations, the expression on interaction potential for hydrophobic effects operating between a spherical particle having hemispherical asperities and a smooth surface, as derived in this study, for rough spherical particle – flat surface geometry,

$$E_{H-RPS} = 2\pi R\lambda_{AB}\Delta G_0(1-\theta)\exp\left(\frac{h_0-h}{\lambda_{AB}}\right) + 4\pi R\varepsilon_S\lambda_{AB}^2\Delta G_0\exp\left(\frac{h_0-h+\varepsilon_S}{\lambda_{AB}}\right) \tag{3.12}$$

which for smooth spherical particle – flat surface geometry becomes,

$$E_{H-PS} = 2\pi R\lambda_{AB}\Delta G_0\exp\left(\frac{h_0-h}{\lambda_{AB}}\right) \tag{3.13}$$

Equation (3.13) is consistent with that obtained by others (Hoek and Agarwal 2006).

3.6 Acknowledgements

The authors acknowledge the Scientific and Technological Research Council of Turkey (TUBITAK) for the financial support provided through the 2214A Scholarship awarded to OG. Adam Drelich provided laboratory assistance during the flotation experiments. JWD would like to express appreciation to Prof. Janusz Laskowski from the University of British Columbia in Vancouver, Canada, for numerous discussions on the role of energy barrier in mineral flotation systems, and to Patrick K. Bowen for his corrections to the manuscript.

4. INTERPLAY OF PARTICLE SHAPE AND SURFACE ROUGHNESS TO REACH MAXIMUM FLOTATION EFFICIENCIES DEPENDING ON COLLECTOR CONCENTRATION

4.1 Introduction

A successful flotation separation requires particles need to possess hydrophobic surfaces which is often dictated by the type and amount of various reagents under suitable conditions. In addition to these parameters, there is a recent upsurge of interest to understand the influence of morphological characteristics on wettability, flotation recovery, and interaction between bubble and particle in flotation system (Ulusoy et al., 2004; Vizcarra et al., 2010; Chiphunfu et al., 2011; Vizcarra et al., 2011; Verelli et al., 2014, Albijanic et al., 2014). Anecdotally, particle shape, especially "angularity" is known to increase the flotation recovery (Vizcarra et al., 2011, Koh et al., 2009), however, such overall tendencies leave it unclear as to the dependence of flotation with particle angularity. Moreover, the effect of roughness is generally correlated with the grinding conditions (Ulusoy and Yekeler, 2005) or etching of spherical particles (Guven et al., 2015, Karakas et al., 2016). However, in real conditions, irregular particles are used as the feed material to flotation processes, and as a result of comminution most particles are rough to a certain extent. In this context, the literature survey given in Table 4.1 clearly demonstrates that, as opposed to well-studied shape factor, roughness has been little studied. Particularly, the combination of both shape and roughness of particles in an isolated manner has never been studied.

In recent years, many papers have been devoted to the flotation of glass beads (Koh et al., 2009, Verelli et al., 2014, Guven et al., 2015, Karakas et al., 2016, Hassas et al., 2016), other industrial minerals like wollastonite, talc and quartz in order to show the effect of morphological features on flotation recoveries (Wiese et al. 2015, Rezai et

[3] This chapter is based on the paper; Onur Guven, Mehmet S. Celik, (2016), Interplay of particle shape and surface roughness to reach maximum flotation efficiencies depending on collector concentrations, Mineral Processing and Extractive Metallurgy Review, (http://dx.doi.org/10.1080/08827508.2016.1218873)

al., 2010, Ulusoy et al., 2003, Kursun and Ulusoy, 2006). In addition, other studies have frequently focused on the effects of flotation parameters like bubble attachment time, collector adsorption, collision efficiency etc. while ignoring the effect of shape factor (Yoon, 2000; Albijanic et al., 2011).

Therefore, in this contribution, ground and abraded glass beads representing various shape and roughness values were produced under controlled grinding conditions, and their flotation behavior was investigated at different collector dosages.

4.2 Experimental

4.2.1 Materials

The spherical glass particles used in this study were standard safety glass spheres with the size of -150+ 106 μm, and -800+250 μm supplied by Potters Industries. The chemical analysis of the sample performed by X-ray fluorescence (XRF) technique revealed that the sample is composed of 72.79 wt% of SiO2, 12.02 wt% CaO, 10.06 wt% Na_2O, 0.83 wt% Al_2O_3, 2.99 wt% MgO, and 0.20 wt% Fe_2O_3. In order to obtain a suitable particle size of -150+106 μm in size, the glass beads of -800+250 μm were wet ground using a ceramic cylindrical mill with 20 cm in diameter and 13112 cm^3 in volume. A mixture of ceramic balls of 30, 25, and 20 mm in diameters which weighed 2810 g was used for the wet grinding. Different grinding times in the range of 1 to 20 min were tested to determine the effect of grinding time on particle morphology and flotation recovery. In each grinding step, all the materials were wet screened through 150 and 106 μm sieves to obtain samples -150+106 μm in size for shape factor, roughness, and micro-flotation studies.Following the grinding, the roughness of glass particles was mainly monitored through controlled abrading processes. In order to obtain different roughness degrees without altering the original size, about 20 g of glass particles were dry mixed with d_{50}= 15 μm fine silicon carbide (SiC) powder (Mohs Hardness Scale: 9) in 50 cm3 Falcon tubes on a mechanical wrist action shaker for 30, 60, 90, and 120 min. The reason for using such fine material was to avoid any further size reduction and alteration of the original shape during the abrasion process. The abraded glass particles were wet screened through a 106 μm sieve, washed with the distilled water several times, dried in the oven, and stored in glass bottles for the flotation experiments.

Table 4.1 : Literature survey of shape factor and roughness related major flotation studies.

Authors	Material Used	Morphology Studied	System(s) studied/application	Salient Finding
Feng and Alrich, 2000	Complex Sulfide Ores	Smoother surfaces from wet grinding Rough surfaces from dry grinding	Effect of grinding conditions on flotation recovery, grade, kinetics, froth stability and adsorption.	1) Higher flotation kinetics for dry ground samples. 2) Froth structure becomes more stable for dry ground samples. 3) Selectivity for dry ground samples was lower compared to wet ground ones. 4) A combination of dry and wet grinding may improve the kinetics and grade of flotation.
Ulusoy et al., 2003	Quartz in different grinding media	Particles of different shape and roughness obtained upon grinding	Comparison of grinding media on shape and use of Zisman equation.	1) High roundness led to low flotation recoveries 2) Wettability increased by roundness and relative width of particles 3) Any increase on roughness increased wettability.
Yekeler et al., 2004	Talc in different grinding media	Different shape and roughness	Evaluation of shape factor on flotation of naturally hydrophobic talc	1) Highly elongated and flat talc particles produced by rod mill decreased critical surface tension or increased flotation recoveries 2) Roughness increased the wettability of talc particles.
Dang-Vu et al. 2006	Glass beads	Smooth and rough glass beads upon etching.	Effect of roughness on contact angle by Washburn method	Effect of roughness was negligible on contact angles of particles contrary to the flat surfaces.
Hicyilmaz et al. 2006	Pyrite particles	Particles of different shape and roughness upon grinding	Effect of roughness and acuteness on flotation recoveries	Lower roughness and acuteness resulted in higher flotation recoveries.
Koh et al. 2009	Borosilicate Glass Beads	Smooth spherical and ground borosilicate glass beads	Effect of sphericity on flotation recovery	Higher flotation rates for ground particles at low surface coverages but an opposite trend was obtained at higher surface coverages.
Rezai et al., 2010	Quartz	Ball mill products of different size ranges	Effect of surface roughness on kinetics of flotation	Finer particle sizes and lower surface roughness values resulted in lower flotation kinetics.
Vizcarra et al., 2011	Chalcopyrite	Irregular chalcopyrite particles ground in laboratory scale hammer mill	Distribution of shape classes in floated products	Angularity comes into prominence only at low floatabilities while it turns out to be the function of collector concentration at higher floatabilities.
Verelli et al., 2014	Borosilicate Glass Beads	Spherical and angular frits	Influence of particle angularity on flotation recovery and induction time.	Reduced induction times were obtained for angular particles; this could be the result of particle shape or orientation of the particles.
Guven et al., 2015	Quartz	Irregular quartz particles after blasting at different nozzle pressures	Effect of sand blasting on morphology and flotation recovery	Higher flotation recovery values were obtained for angular and rough particles as a result of blasting.
Guven et al., 2015	Glass Beads	Spherical and rough glass particles after abrading and etching with HF	Effect of roughness on flotation kinetics and theoretical modelling of bubble-particle interactions	1) Rougher particles caused higher flotation kinetics rate. 2) Lower energy barriers were calculated even at nano-sized roughness values and correlated with the experimental findings.
Wiese et al. 2015	Ballotini Talc Vermiculite Mica Wollastonite	Particles of different aspect ratios	Particles with different shapes exhibited different entrainment properties.	1) Particles of different aspect ratios showed different entrainment properties. 2) While near spherical and elongate particles reported less entrainment, particles with a less well-defined shape followed the same trend.
Little et al., 2015	Chromite	Irregular chromite particles after communition in different mills	Particle shape characterization by Auto-SEM method.	1) Influence of breakage mechanism in different mills were quantitatively demonstrated 2) Roundness and aspect ratio were found the most suitable parameters for characterization of fine particles.
Karakas et al. 2016	Glass Beads	Spherical and rough glass particles after etching.	Determining the surface forces between HTAB and particles upon roughness degrees	1) Flotation recoveries increased to an extent of roughness degree at the same collector concentration 2) Higher adsorption affinity was observed for rough spherical particles.

All the glass particles were repeatedly washed following a procedure given in the literature (Koh et al., 2009) in order to prevent the effect of organic and inorganic contamination during the flotation tests. In this procedure, the particles were treated with 2.5 v/v% H_2SO_4 followed by 2.5 w/v% NaOH solutions, and then washed with distilled water until a constant pH value of 7.3 was obtained for the glass beads. Finally, the slurry was subsequently filtered and dried at 105 ºC in an oven overnight.

4.3 Methods

4.3.1 Morphological Characterization

The shape factors and roughness parameters of the ground and abraded glass beads were determined using the images obtained with a binocular microscope of ×500 magnification and analyzed by Image Analysis and profilometer. For the shape factor analysis of the particles, Leica QWin Image Analyze software (Leica Qwin User Manual, 1995) was used based on particle projections obtained from the micrographs of particles. The roundness and roughness values required to evaluate flotation recoveries were obtained as follows: The value of roundness parameter was automatically calculated for about 200 particles by adapting the equation given below (Forrsberg and Zhai, 1985):

$$\text{Roundness (Ro)} = \frac{4\pi A}{P^2} \tag{4.1}$$

where P is the perimeter of a particle and A is the area evaluated by the software. In literature, the same equation was also used for defining the “Circularity” term (Little et al., 2015). However we adapted this equation for the definition of roundness from Forrsberg and Zhai, 1985 as cited in Ulusoy et al. 2003. And the characterization of particle morphology constitutes an important role for determining the interactions between particles and particle-bubble in systems in flotation (Guven et al., 2015).

The surface roughness of the ground and abraded particles at different times were determined with a Zeiss Axio CSM700™ Optical Profilometer device. In this instrumental analysis, the roughness evaluation is based upon the differences between profile heights for each particle selected on the image obtained by the camera. The particles were mounted on glass slides through double sided adhesive tapes were

prepared for convenience. Roughness characterization included average roughness (Ra) represented the average of absolute values for surface heights deviations.

4.3.2 Micro-flotation experiments

The micro-flotation tests were carried out using a 150 cm^3 micro-flotation column cell (25×220 mm) with a ceramic frit (pore size of 15 μm) which was mounted on a magnetic stirrer as described elsewhere (Hancer and Celik, 1993). A commercial reagent namely Flotigam EDA (Clariant), an alkyl ether propylene amine with a chemical formula R-O-$(CH_2)_3$-NH_2, partially neutralized with acetic acid (amine salt) was used as a collector. In addition, Methyl isobutyl carbinol (MIBC) was used as a frother. One gram of -150+106 μm glass particles were conditioned in desired concentrations of collector solutions for 5 min. The pH value of the pulp measured as 7.3±0.1 did not change significantly during the flotation. High purity nitrogen gas was used for the aeration at a rate of 60 cm^3/min. The amount of both float and sink products was determined gravimetrically. It is worth to mention that all experiments were repeated three times, and the average flotation recovery value for each test was separately calculated and illustrated in relevant Figures.

4.4 Results and Discussion

4.4.1 Morphological features of particles

In order to determine the effect of grinding and abrasion times on shape and roughness indices of glass beads, a morphological characterization was performed before the flotation tests. Figure 4.1 illustrates the schematic drawings of the representative micrographs for the spherical particles through the grinding (milling) and the roughening (abrading) stages. The morphological features of the particles reveal that the edges of the particles were gradually chipped off as the grinding time proceeded to 5 min, and the roundness values decreased to 0.773 from 0.996. However, after the grinding time of 5 min, the variations in the roundness remained as 0.780±0.020. Following the grinding process, the irregular shaped glass beads were subjected to the abrasion process using SiC powder to allow the particles only undergo a mild roughening. It is worth to note that the abrasion process for the ground particles induced only a negligible difference in the roundness of the particles in the range of 0.801± 0.005.

In the literature, numerous papers have been published to show the effects of different grinding media on particle morphology in terms of their shape factor and roughness (Ulusoy et al., 2004, Rezai et al., 2010, Feng and Aldrich, 2000). However, in these studies, both of these factors were investigated for specific particle size ranges and shape factor obtained after a certain grinding time while this kind of approach has masked the distinction between shape and roughness. In this respect, these results, to our knowledge, are the first reported in the literature.

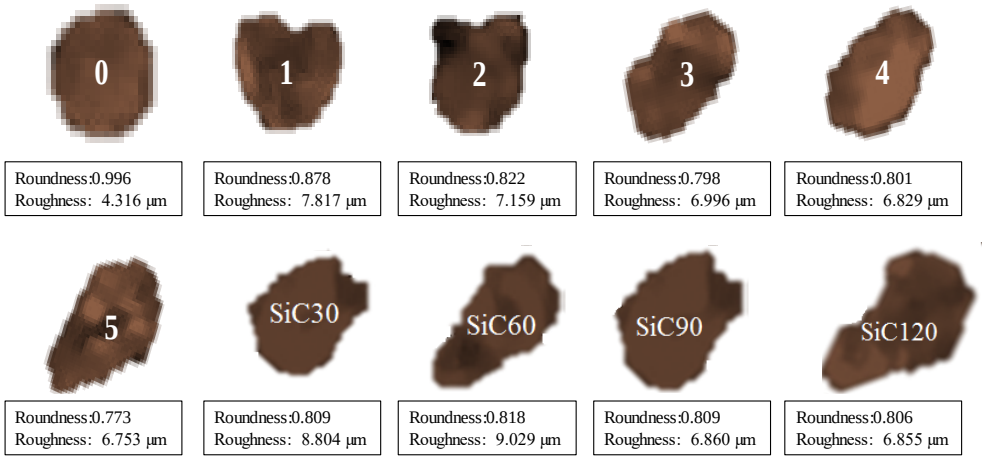

Figure 4.1 : Schematic envelope of particles as a function of grinding and abrasion times.

In addition, the roughness of the material increased from 4.316 µm to 7.159 µm until 2 minutes of grinding time and then a gradual decrease was obtained down to 6.753 µm at 5 minutes of grinding time. This decrease after 2 minutes grinding can be attributed to the removal of debris due its interaction with water in line with the observations reported by Feng and Aldrich (2000). During the abrasion process carried out at 30, 60, 90 and 120 minutes, however, the roughness increased to 9.029 µm upon roughening (SiC60) and then decreased again to 6.855 (SiC120). Figure 4.2 presents the 3-D images of representative particles plotted using Interactive 3D Surface Plot Plugin by Image J software.

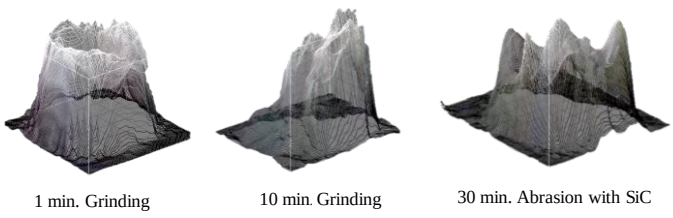

Figure 4.2 : 3-D plots of representative particles with Image J.

The above findings made it possible to investigate the effect of shape factors and roughness independently to identify their individual effects as a function of collector concentrations or implicitly hydrophobicity of particles.

4.4.2 Micro-flotation experiments with ground and abraded particles

Figure 4.3 presents the results of a series of micro-flotation tests carried out with spherical, ground, and abraded particles as a function of three collector concentrations at natural pH of 7.3. The results showed that while the flotation recovery was 23.6% at 1×10^{-6} M collector concentrations at a natural pH of 7.3 for the spherical particles, it increased to 31.3% and 39.4 % for the ground and abraded particles, respectively. The similar trends were also obtained at higher collector concentrations. For instance, while 39.0% of flotation recovery was obtained at 1×10^{-4} M collector concentration for the spherical particles, 50.3% and 52.7% were obtained for the ground and abraded particles. However, at 10^{-3} M collector concentration, while the difference between the floatability of ground and spherical one increases significantly, that between the floatability of abraded and ground ones almost ceases. Thus, at 1×10^{-3} M collector concentration, the recovery increased to 71.4 % for the spherical particles whereas 88.4 % and 88.7 % for the ground and abraded particles, respectively.

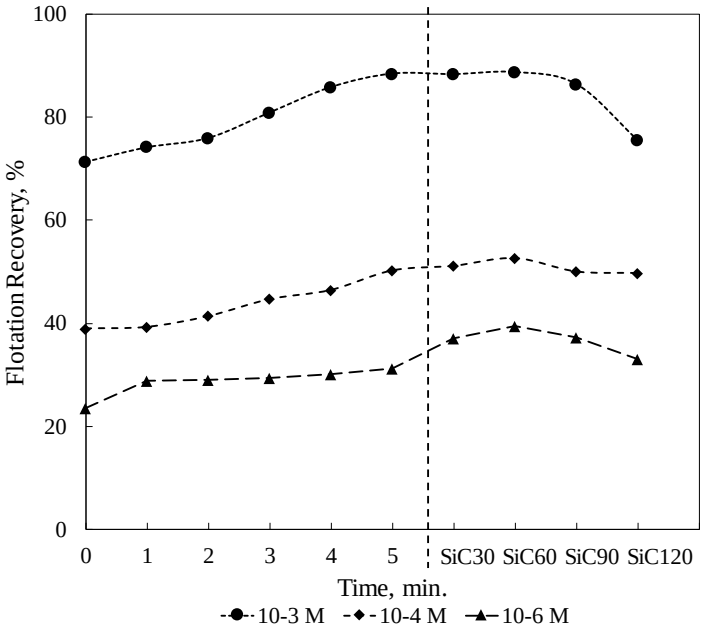

Figure 4.3 : Effect of grinding and abrasion times on flotation recovery of glass beads at three levels of collector concentrations.

In the light of these findings, morphological character of particles on bubble-particle interactions and its eventual effect on flotation recoveries was thoroughly investigated for the particles conditioned at the three levels of collector concentrations, i.e. 10^{-6}, 10^{-4}, and 10^{-3} M.

Figure 4.3 also shows a gradual increase in flotation recovery upon increasing the grinding time up to the maximum roughness value; this can be definitively ascribed to the combination of morphological changes involving shape and roughness in this particular system.

In view of these findings, the lowest concentration of 1×10^{-6} M was selected in order to distinguish the contribution of the extent of shape and roughness on flotation recoveries.

4.4.3 Correlation between morphological features and flotation recoveries

The results of micro-flotation tests at $1x10^{-6}$ M clearly showed that the lowest flotation recovery values were obtained with spherical particles at the highest roundness value of 0.996 and roughness value of 4.316 μm. Such finding for spherical particles was in line with the findings of Verelli et al. (2014).

Figure 4.4 illustrates the flotation behavior of the glass beads at $1x10^{-6}$ M collector concentration as a function of the grinding and abrasion times. This finding for tracing the shape factor up to 5 min through ball milling, and then maintain the same shape factor while inducing roughness on the particles. As previously shown in Figure 1, the profilometer measurements showed that the roughness of ground particles increased from 6.753 μm to 9.029 μm after the abrasion time of 60 min. Thus, roughness measurements above 60 min. abrasion time indicated a significant decrease down to 6.855 μm which was also correlated with the flotation recoveries in Figure 4.4.

Thus, after the grinding, a gradual increase was obtained in the flotation recoveries which are directly proportional to the decrease on roundness values though the particles were rough to a certain extent. These results also showed that the efficiency of flotation was inversely proportional to the roundness value of particles. Similar trends were also presented in the literature. For instance, Ulusoy et al. (2003) showed that after grinding quartz in ball, rod and autogenous mills, the products of rod mill resulted in higher flotation recoveries due to their lower roundness values. Likewise, in another study of the same group, similar trend in grinding was also found for other

industrial minerals as barite, calcite and talc (Ulusoy et al., 2003, Ulusoy and Yekeler, 2005, Yekeler et al., 2004) which then demonstrated the influence of grinding media. Apart from grinding processes, in our previous paper, a similar trend was obtained for the blasted quartz particles where lower roundness values exhibited higher flotation recoveries (Guven et al., 2015). And to our knowledge, the importance of grinding time on particle shape and correspondingly flotation recoveries were quantitatively shown for the first time. However, the roughness values given in Figure 4.1 also indicated that upon increasing the wet grinding times, smoother particles were obtained. As mentioned in the previous sections, this finding could be attributed to the better removal of very fine particles (debris) on glass beads which may influence the roughness of particles.

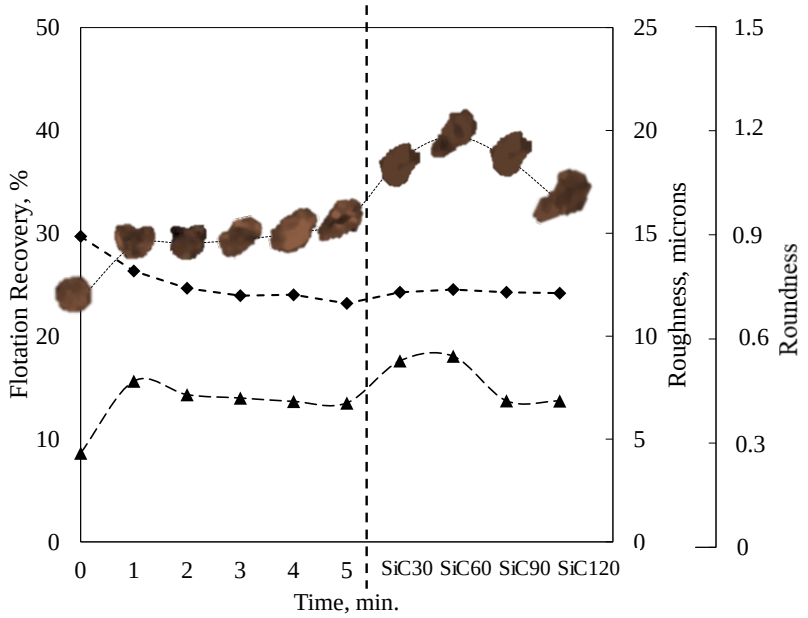

Figure 4.4 : Flotation behavior of glass beads at $1x10^{-6}$ M amine collector as functions of grinding and abrasion times.Roundness and roughness of particles are also given to correlate flotation recoveries with their morphology.

The data given in Figure 4.3 were utilized to better illustrate and also isolate the effect of shape from that of roughness. The shape effect was obtained by taking each flotation recovery value at a particular collector concentration at a given grinding time (in this case 5 min. grinding time) and subtracting from the base recovery value for spherical particles, viz. ground-spherical. Similarly, the roughness effect was obtained by taking each flotation recovery value at a particular collector concentration at a given

roughening time (corresponding to maximum roughness value) and subtracting from the base recovery value for spherical particles, viz. abraded-ground at 5 min.

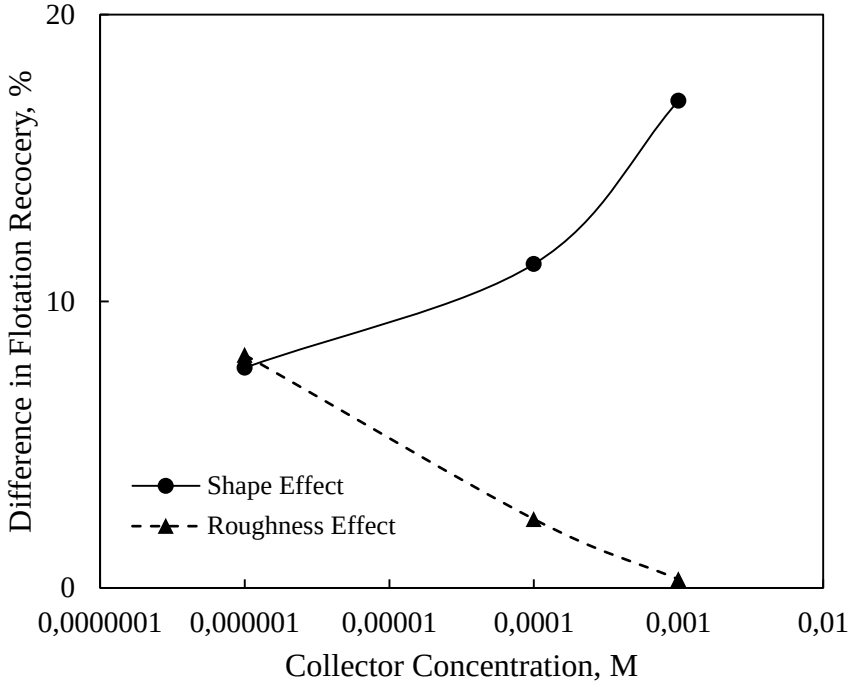

Figure 4.5 : Comparison of shape effect (% Recovery at 5 min. Grinding – % Recovery at 0 min. grinding) of particles against roughness effect (% Recovery value at SiC60 – % Recovery at 5 min. grinding) as a function of collector concentration (values taken from Figure 4.1).

Figure 4.5 shows the flotation recoveries vs. collector concentration for shape and roughness effects. The results vividly demonstrate that shape effect is enhanced upon increasing collector concentration from $1x10^{-6}$ to $1x10^{-3}$ M. Conversely, the roughness effect deteriorates with increasing the collector dosage from $1x10^{-6}$ to $1x10^{-3}$ M. In other words, at high collector coverages the flotation recoveries are dominated by shape factor alone. As it is well known, the higher angularity may result in lower induction times and consequently in higher flotation recoveries (Verelli et al., 2014). However, at low collector dosages, the roughness level is of paramount importance for bubble-particle capture. High speed camera pictures are in progress to further verify these results.

4.5 Conclusions

The findings from this study provide a major breakthrough considering the controversial effect of shape and roughness of particles reported on flotation recoveries. The dependence of morphology of particles has a direct relationship with

the hydrophobicity of particles and in turn on flotation recoveries. While the effect of shape factor is most significant at high collector concentrations, that of roughness is diminished at high hydrophobicities. The morphological features presented in this study may be beneficially tuned to grinding conditions to achieve optimum flotation results.

5. DEPENDENCE OF MORPHOLOGY ON ANIONIC FLOTATION OF ALUMINA

5.1 Introduction

In recent years, morphological properties come into prominence for explaining flotation recoveries of different particles like talc (Kursun and Ulusoy, 2006), quartz (Ulusoy et al., 2003, Rezai et al., 2010, Guven et al., 2015), particles of different aspect ratios including wollastonite (Wiese et al., 2015), barite, calcite (Ulusoy et al., 2004), glass beads (Koh et al., 2009, Guven et al., 2015, Karakas et al., 2016, Hassas et al., 2016), complex sulphide ores (Feng and Aldrich, 2000) and anthracite (Wen et al., 2015). As mentioned in a recent review, these variations can be addressed in two main classes of surface morphology such as "Shape factors" and "Roughness" (Mahmoud, A., 2009). In most of these publications, increase in flotation recoveries for many types of minerals was attributed to a decrease in Roundness parameter. This general finding was also proven by recent investigations (Verelli et al., 2014, Hassas et al., 2016) in terms of bubble-particle attachment and induction times. Apart from the effect of roundness, some investigations also involved only surface roughness effect for the evaluation of overall flotation results (Ducker et al., 1989, Feng and Aldrich, 2000, Guven et al., 2015, Hassas et al., 2016,). In most of these studies it was found that the presence of roughness leads to some enhancement in flotation recoveries in terms of both experimental data and theoretical assumptions. However, apart from smooth spherical particles, one cannot only induce either shape or roughness on a particle through grinding process. Thus a careful procedure is required to isolate the effect of shape from roughness in order to interpret hydrophobicity dependent flotation recoveries. The studies on alumina flotation with SDS mostly focused on the effects of pH and adsorption of SDS onto alumina particles (Somasundaran and Fuerstenau, 1966, Fuerstenau and Pradip, 2005, Adak et al., 2005). The effect of surface

[4] This chapter is based on the paper; " Onur Guven, Fırat Karakas, Nurgül Kodrazi, Mehmet S. Celik, (2016) "Dependence of morphology on anionic flotation of alumina", International Journal of Mineral Processing, http://dx.doi.org/10.1016/j.minpro.2016.06.006 0301-7516/

morphology, to our knowledge, has never been considered in the flotation of alumina particles. Thus in this study, different morphology modification procedures as grinding and abrasion were applied to induce changes on shape and roughness of alumina particles followed by flotation in the presence of SDS.

5.2 Experimental Studies

5.2.1 Alumina Particles and their preparation

Aluminum oxide particles -106+74 μm in size were supplied by ETI Aluminum Industries, Turkey. The pre-analysis of the sample performed by X-ray fluorescence (XRF) technique revealed that the sample was composed of 99.1 % of Al_2O_3, 0.01 % SiO_2, 0.008 % Fe_2O_3, 0.15 % Na_2O and 0.007 % CaO per weight. The average B.E.T surface area of the delivered sample (with d_{50} size of 75 μm) is 80 m^2/g.

In order to obtain particles with -74+53 μm in size for use in flotation studies, a mixture of ceramic balls of 30, 25, and 20 mm in diameters which weighed about 816 g was used in a cylindrical ceramic mill of 13112 cm^3 under wet conditions. The reason for selecting a low ball charge in this mill design was to reduce overgrinding of relatively close feed size of -106+74 μm. Different grinding times in the range of 30 seconds to 10 minutes were tested to determine the effect of grinding time on particle morphology and in turn flotation recovery. Thus, in each grinding step, all the materials were wet screened through 74 and 53 μm sieves to obtain samples in -74+53 μm size for both micro-flotation studies, shape factor and roughness analysis.

For roughening the alumina surfaces without altering the original size, about 5 g of alumina particles were dry abraded in 22 cm^3 test tubes and mixed on a mechanical wrist action shaker in the presence of 1 g fine silicon carbide (d_{50}; 15 μm (Mohs Hardness Scale: 9.0-9.5) for 30, 60, 90, 120, 450, 600 and 1440 minutes in order to obtain particles with different roughness degrees. The reason for using such fine material was to avoid any size reduction during abrasion process. After each abrasion test, the abraded alumina particles were wet screened through a 53 μm sieve for controlling the particle size fed to flotation process and also for removal of silicon carbide from alumina surfaces. All the materials were water washed several times, dried, and stored in nylon bags.

5.2.2 Morphological Characterization of Particles

5.2.2.1 Image Analysis

Ground and abraded alumina particles were imaged with a binocular microscope of 50X magnification, where Roundness of particles was determined by Image Analysis technique. For shape factor analysis, Image J software (Free of License) was used based on particle projections obtained from the micrographs of particles. The processing of the images simply based on taking the threshold of each picture as to automatically select the particles with the color difference. In our previous studies, a different software namely Leica QWin Image Analyzer was conducted for shape factor analysis (Guven et al., 2014, 2015[b]), however in order to decrease the tolerance of human based error and due to the finer size range of the particles, Image J software was selected for shape analysis. The advantage of using this software was the ability to evaluate more particles for shape factor analysis which produces more reliable results on shape factor. The Roundness values required to evaluate flotation recoveries were obtained as follows.

$$\text{Roundness (Ro)} = \frac{4\pi A}{P^2} \qquad (5.1)$$

Where P is the perimeter and A is the area of particle evaluated by the software.

5.2.2.2 Roughness Analysis

The roughness degree of both ground and abraded alumina particles at different times were determined by Zeiss Axio CSM700TM Optical Profilometer device. In this instrumental analysis, after imaging of particles by binocular microscope with 20X magnification, the roughness evaluation was made on the threshold of these images. The analysis was made based on the differences between profile heights for each selected area on particles. Roughness characterization included average roughness (Ra) and other roughness parameters such as skewness (Rsk), kurtosis (Rku), however only average roughness value which presents the average of absolute values for surface heights deviations was considered in the evaluation of flotation recoveries as a function of roughness values. It is worth to note that at least 10 particles were selected and the average values of these measurements were used and presented. The procedure for roughness measurement is shown in Figure 5.1.

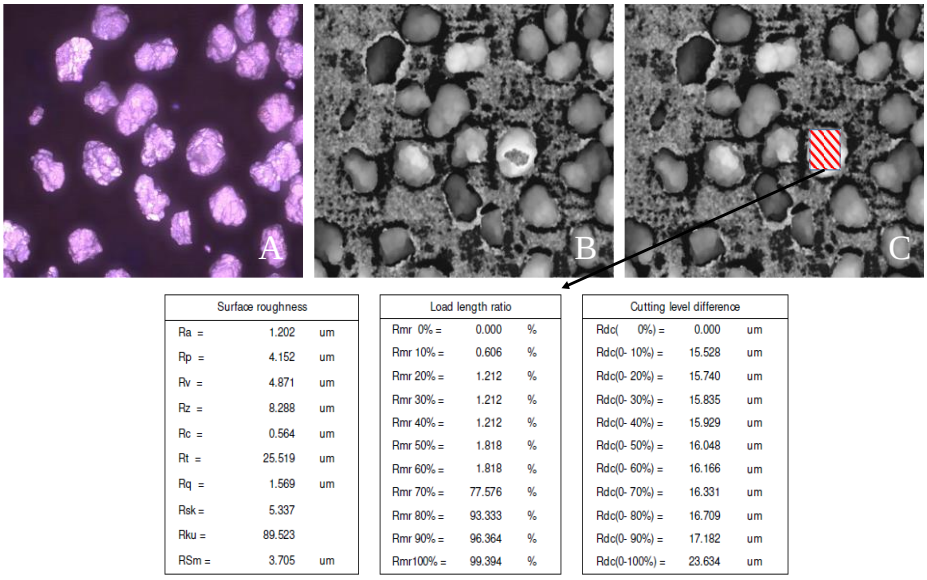

Figure 5.1 : Procedure of roughness measurement by optical profilometer (a) Raw image of particles, (b) Threshold presentation of the raw images, (c)Area selection for roughness measurement).

5.2.3 Micro-flotation Experiments

The micro-flotation tests were carried out using a 150 cm^3 micro-flotation column cell (25×220 mm) with a ceramic frit (pore size of 15 ìm) which was mounted on a magnetic stirrer as described elsewhere (Hancer and Celik, 1993). Moreover, an additional feed unit with 10 cc volume was used in order to stabilize the washing water for flotation. Sodium dodecyl sulfate (SDS) ($C_{12}H_{25}NaO_4S$, M, 288.38 g) with ≥ 98.0 % GC was supplied from Fluka Company and used as collector. In addition, throughout all flotation tests, 40 ppm MIBC (Methyl isobutyl carbinol) was used in order to stabilize the froth. During flotation, 1 g of alumina particles in -74+53 μm size was conditioned in collector solutions of desired concentrations for 3 min. The pH value of the medium was measured as 6.48±0.1. High purity nitrogen gas was used for aeration to maintain gas flow at a rate of 50 cm^3/min throughout all the entire flotation experiments. The amount of both float and sink products was determined gravimetrically. Besides micro-flotation experiments, the bubble particle interactions were also monitored by fast cam instrument where three types of particles, i.e. original (relatively spherical), ground (angular) and abraded (rougher) have been used. A similar procedure was followed throughout the monitoring experiments where the particles were introduced into a small beaker of water prior to the experiment (Verelli et al. 2011). Then a aliquot of particles was sucked up using a Pasteur pipette and transferred to a second pipette which was truncated with knife for use as orifice. The

bubble was generated with atmospheric air which is blown from a 2 ml syringe with a needle bent in order to provide horizontal capillary rise. A schematic presentation of the system is provided in Figure 5.2.

The liquid medium was $9.76x10^{-5}$ M SDS solution which was contained in a glass-walled tank with 26 x 76 mm in size. The interactions were recorded on a Photron Ultima Fastcam high-speed video camera operating at 2000 frames per second). Video recordings were processed using the Photron Fast Cam Viewer software.

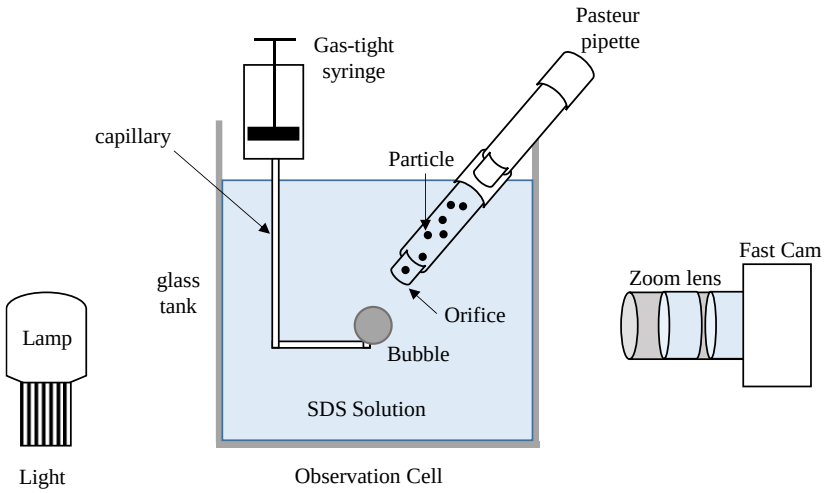

Figure 5.2 : Schematic presentation of the particle dropping apparatus.

5.3 Results and Discussion

5.3.1 Morphological Characterization of Ground and Abraded Particles

In Figure 5.3, the roundness and roughness values of both ground and abraded particles are presented under representative pictures taken from micrographs. Compared to glass beads produced under similar conditions (Guven and Celik, 2015), the range of variation in shape factors is not wide for alumina particles according to their initial irregular structure. The roundness value was found to vary in the range of 0.876-0.811 for ground and abraded particles at different treatment times.

The evaluation of roughness can be divided into two regions as grinding and abrasion. In the first region, besides the variation of roundness values, the roughness of particles changes between 0.707 μm to 0.524 μm in the first two minutes and then progressively increased to 0.680 μm after 5 minutes. This characteristics of the material can be explained with the increasing amount of the debris adhered to the particles that produces height variations on surfaces. In the second region, the roughness of particles

increased from 0.690 µm up to 1.074 µm upon abrasion for 60 minutes (SiC60), however a critical decrease was obtained in the time span of SiC120-SiC450 to 0.720 µm. In addition, at abrasion times higher than 450 minutes which is denoted as SiC1440, the roughness of particles increased to 0.906 µm whereas the roundness value remained constant as 0.834.

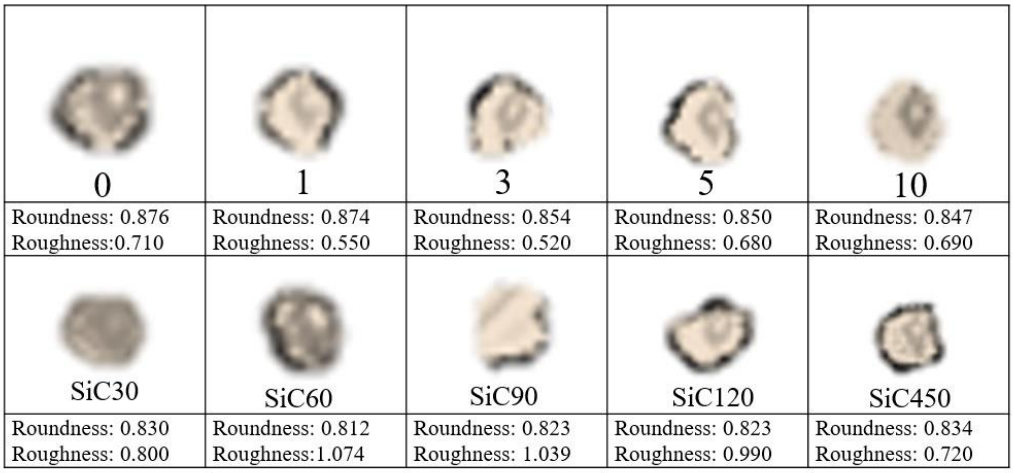

Figure 5.3 : Schematic envelope of particles as a function of grinding and abrasion times.

It is worth to note that the use of silicon carbide for roughening the surfaces of alumina particles is not effective compared to that of glass beads (Guven and Celik, 2015). This can be related to their close hardness values on Mohs scale which are 9.0 and 9.5, respectively. Thus, the roughness of alumina particles varies from 0.520 to 1.074 µm whereas this range was reported for glass beads in between 4.316 to 9.029 µm.

In literature, plethora of research was conducted to illustrate the effects of different mechanisms like grinding (Ulusoy et al., 2004, Rezai et al., 2010, Feng and Aldrich, 2000, Wiese et al., 2015), etching (Dang-Vu et al, 2006), abrasion (Guven et al., 2015[a]), blasting (Guven et al., 2015[b]) on different shape factors and roughness. As mentioned in the "Introduction" section, most of these studies demonstrated that upon decreasing roundness, higher recoveries could be obtained. However, we earlier addressed the methodology to distinguish these parameters on particulate systems (Guven and Celik, 2015). Thus, an extended discussion about the effect of morphology on flotation recoveries will be conducted in the proceeding section.

5.3.2 Micro-flotation experiments with ground and abraded particles

The micro-flotation test results in Figure 5.4 indicated that the flotation recovery was about 10 % at $1.06x10^{-5}$ M SDS concentration, then increased to 80 % at $1.06x10^{-3}$ M SDS concentration and finally reached the plateau above this concentration. The results of this study are consistent with the findings in the literature (Somasundaran and Fuerstenau, 1966) where the critical micelle concentration of SDS was reported as $5x10^{-3}$ M (Fuerstenau and Pradip, 2005). Due to the well-known pH dependence on the interactions of alumina with SDS (Somasundaran and Fuerstenau, 1966), the pH value was kept constant at the natural pH of 6.48±0.03. In addition, the flotation recoveries are in line with the findings presented in literature (Modi and Fuerstenau (1960) and Fuerstenau and Modi (1959).

In Figure 5.5, the results of a series of micro-flotation tests carried out with original, ground and abraded particles are presented as a function of four different collector concentrations at natural pH of 6.48.

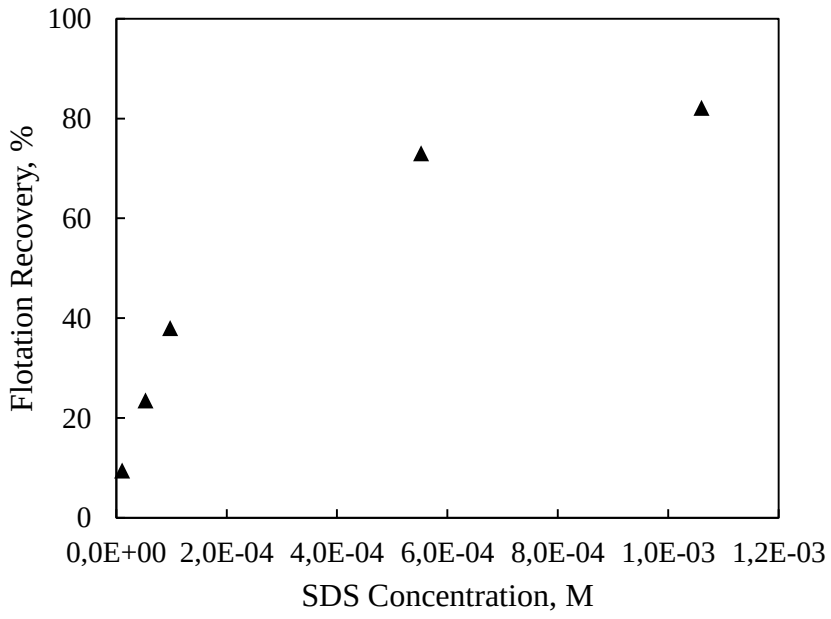

Figure 5.4 : Micro-flotation response of alumina particles as a function of SDS concentration.

As shown in Figure 5.5, while the recovery at $1.06x10^{-5}$ M SDS concentration was 9.48 % with the original particles, it increased to 19.7 % and 20.9 % for the ground and abraded particles, respectively. At higher collector concentrations of $5.29x10^{-5}$ and $9.76x10^{-5}$ M, the flotation recoveries for the original particles were 23.56 and 38.01 %, respectively. Thus after 10 minutes of grinding, the recoveries obtained under these

concentrations increased to 36.8 and 41.7 %, respectively. The results of flotation tests for glass beads earlier revealed that while the recoveries were shape dependent at higher collector concentrations, they were roughness dependent at lower collector concentrations (Guven and Celik, 2015). Likewise, in this study the difference between recoveries at lower concentrations can well be attributed to the small differences found on roughness values of alumina particles upon abrasion process shown in Figure 5.3. Thus, the difference between flotation recoveries of ground and abraded particles of 18.28 % is higher for $9.76x10^{-5}$ M SDS concentration whereas it remained at 4.9 % for $5.29x10^{-5}$ SDS concentration which are all in line with the afore-mentioned statements on flotation recoveries. At $5.52x10^{-4}$ M concentration, the difference between the floatability of original and ground particles increases in accord with the variation of shape factors in particular "Roundness" values where the difference on floatability of ground and abraded particles ceases. Thus at $5.52x10^{-4}$ M collector concentration, the recovery was 73.1 % for the original particles whereas 79.9 % and 88.2 % for the ground and abraded particles, respectively.

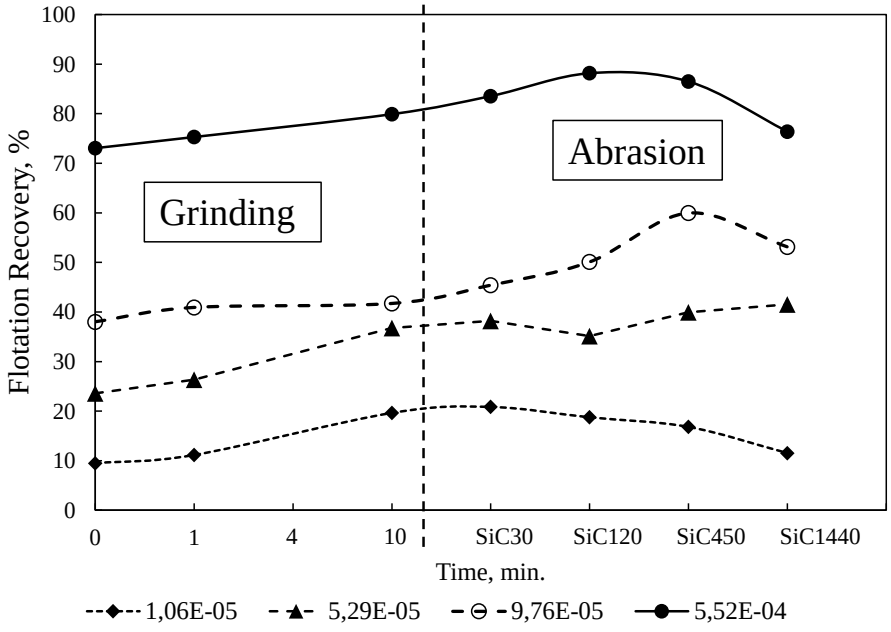

Figure 5.5 : Micro-flotation response of alumina particles as a function of grinding and abrasion times.

As mentioned in the "Methods" section, the same trend for the bubble-particle interactions was also found with particles of different shape factors and roughness values. The concentration of $9.76x10^{-5}$ M SDS in the suspension was selected on the basis of micro-flotation tests given in Figure 5.5. Three different states of particles, as

given in the video supplementary files, were considered in this analysis. (i) particles ground for 1 min. shown in Figure 5.3 labeled as 1 (Ro: 0.874, Rs: 0.550). In this test, very few particles were observed to have the contact with the air bubble. Considering the irregular shape of alumina particles, they were observed to attach to the bubble along their longest edges. (ii) particles ground for 10 minutes shown in Fig 5.3 labeled as 10 (Ro: 0.847, Rs:0.690). In this case, the particles were found to acquire more angular shape and somewhat rougher surfaces. And thus similar to Part (i), they were observed to attach to the bubble along their longest edges. Interestingly, the particles were observed to exhibit coagulation tendency; the number of particles in contact with bubble became considerably higher than particles in Part (i). (iii) particles abraded for 90 minutes shown in Figure 5.3, labeled as SiC90 (Ro: 0.823, Rs: 1.039), demonstrated more rougher surfaces and higher coagulation tendency forming clusters. These results corroborate our unpublished findings that rougher surfaces are more akin to coagulation. It is also our future aim to verify if particles coagulate before they hit the air bubble particularly in the region of hemi-micelle formation.

5.3.3 The relation between morphological features and flotation characteristics

The results of micro-flotation tests at 9.76×10^{-5} M clearly showed that the lowest flotation recoveries were obtained with the original particles at the highest roundness value of 0.876, and roughness value of 0.707 μm. As mentioned in the previous section, the micro-flotation test results for the original particles are all in line with the findings in the literature (Modi and Fuerstenau, 1960, Fuerstenau and Modi, 1959). In Figure 6, the flotation characteristics of alumina particles are shown as a function of grinding and abrasion times. Similar trend was also obtained in our previous study with quartz (Guven et al. 2015[b]) where decreasing roundness values with nozzle pressure yielded gradual increase in flotation recoveries. In addition, the same trend was also obtained between floatability and roughness of quartz particles. Thus, the differences on roughness values were reasonably higher leading to significant increases on recovery values. Likewise, Ulusoy et al., (2005) also suggested that the floatability of industrial minerals like barite, calcite, quartz and talc may increase in the presence of angular particles obtained by ball mill.

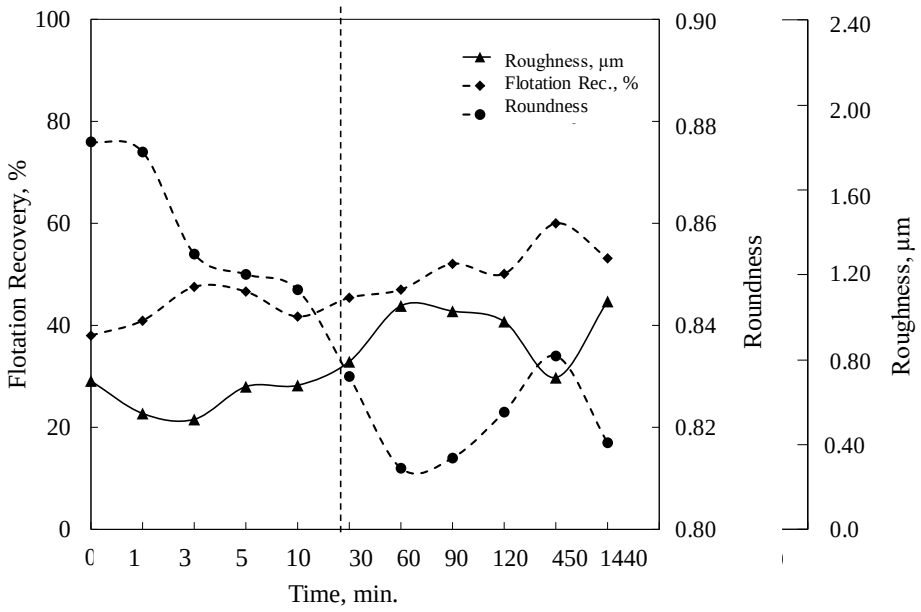

Figure 5.6 : Flotation behavior of alumina particles at 9.76x10-5 M SDS collector as functions of grinding and abrasion times. Roundness and roughness of particles are also given to correlate flotation recoveries with their morphology.

However, the results of the same team also suggested that upon increasing roughness degrees, the floatability of minerals will be reversely affected; this was explained by Zisman's approach (Zisman, 1964). However as discussed in our previous paper (Guven et al., 2015[b]), the use of a broad size range of particles (45-250 µm) could influence the morphological properties and hence flotation recoveries. Considering this finding, in this study, a narrow size range of -75+53 µm was used during both flotation and morphological analysis. However, the variation on roughness and shape factors is not proportional compared to those previously obtained for glass beads. As mentioned above, this can be attributed to the structural differences. Thus the compact differences in roundness and roughness values is not as large as glass beads according to the hard structure of alumina which then complicated both grinding and abrasion process (Guven and Celik,2015). The effects of shape factor and surface roughness on flotation recoveries were also presented by high speed digital video recordings on some recent publications (Verelli et al., 2014, Hassas et al. 2016). Of these, Hassas et al. (2016) also suggested that lower induction times and in turn higher flotation recoveries may be obtained in the case of angular glass bead particles in line with our assumptions for the flotation of alumina particles. From this point of view, our results on enhanced flotation recovery as a function of shape factor and roughness values are all in agreement with the previous literature findings.

The data given in Figure 5.7 were utilized to better illustrate and also isolate the effect of shape from that of roughness. The shape effect was obtained by taking maximum flotation recoveries at a particular collector concentration at a particular grinding time (in this case 10 min. grinding time) and subtracting from the base recovery value for original particles, viz. ground-original. Similarly, the roughness effect was obtained by taking each flotation recovery values at a particular collector concentration for a given roughening time (corresponding to maximum flotation recovery), and subtracting them from the recovery value for ground particles, viz. abraded-ground at 10 min.

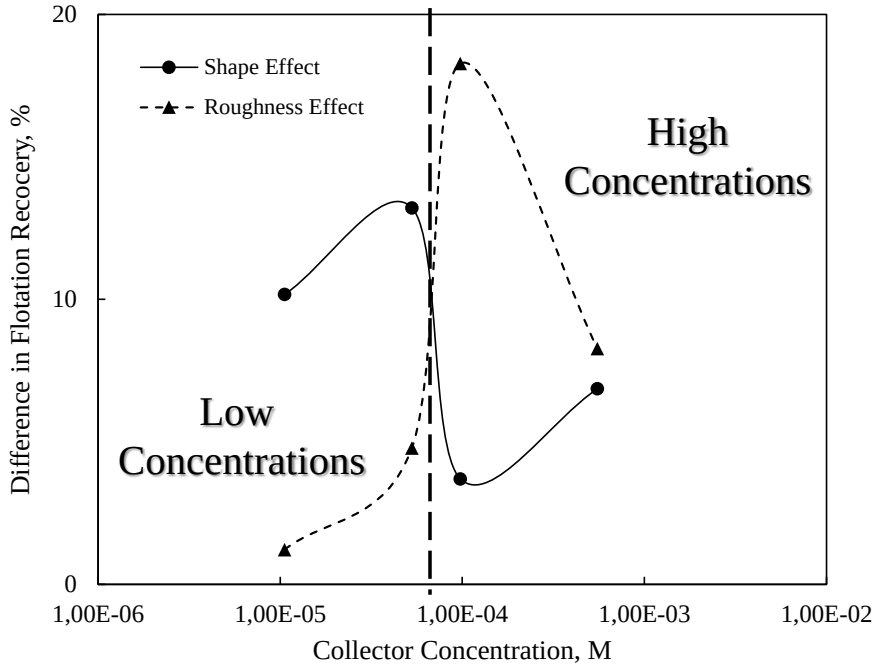

Figure 5.7 : Comparison of shape effect (Max. % Recovery at any Grinding time– % Recovery at 10 min. grinding) of particles against roughness effect (Max. % Recovery at any abrasion time– Max. % Recovery at Grinding) as a function of collector concentration (values taken from Figure 5.5).

The results shown in In Figure 5.7 at "Low Concentrations" partly demonstrated that the both roughness and shape equally raise flotation recoveries. In other words, for SDS concentrations such as 1.06×10^{-5} and 5.29×10^{-5} M, while the difference between the maximum flotation recovery values was 3.04 % for shape factors, it was 3.57 % for roughness. While roughness effect continues to dominate flotation recoveries even at moderate concentrations, shape effect relatively diminishes at the same concentration range. However at high concentration of 5.52×10^{-4} M, while the shape factor has an enhancing effect on flotation recoveries, roughness has a negative effect.

The following two explanations can be afforded: (i) the change in both shape (the range is 0.05) and roughness (the range is 0.5 μm) values in alumina is rather low compared to those (shape range 0.2; roughness 4.7 μm) for glass beads; this makes the difference in recovery particularly at this relatively extreme concentration rather low, (ii) surface coverage in glass bead/amine system at about pH 6.5 is relatively low, however, in alumina/SDS system at the same system pH and 10^{-3} M concentration is comparatively high. This is also expected to induce lower hydrophobicities and lower differences in flotation recoveries of alumina/SDS system.

5.4 Conclusions

The findings in this study provide a systematic analysis on the flotation of irregularly shaped alumina particles. A detailed correlation was made between the roundness, roughness and flotation recoveries. Thus, the dependence of shape on alumina particles showed that upon chipping off the round corners of alumina particles, they become more angular and resulted in higher flotation recoveries. While the dependence of roughness on alumina particles continues to enhance flotation recoveries up to moderate SDS concentrations but declines at higher SDS addition. High speed camera pictures taken in alumina-SDS suspensions also indicated that the coagulation tendency was enhanced due to increasing roughness of particles. This was found to improve the bubble-particle attachment.

6. CONCLUSIONS

The main hypothesis addresses in this thesis was “Because particle morphology is one of the misunderstood issues for assessing the success of flotation process and interactions between particles and bubbles, its determination and modelling through various measurements along with micro-flotation tests are necessary to identify the mechanisms responsible for it”.

The first sub-hypothesis in this thesis was that besides many shape factors, deviation from roundness is likely to be the driving force at the same hydrophobicicty of particles modified through collector addition. To validate this sub-hypothesis irregular shaped particles were produced using different methods like grinding and blasting while the particle size was kept constant in all experiments. When considered, all the flotation recoveries were in line with the roundness values measured for all systems as glass-amine and alumina-SDS systems at higher hydrophobic degrees. Also, induction time and bubble-particle attachment efficiencies decreased in proportion to the roundness value of particles which also showed its significant role of morphology in determining the interaction between particles and bubles. On the other hand, the contact angles also increased with decreasing roundness values which also suggested enhanced hydrophobicity for these systems. The second sub-hypothesis in this thesis was that roughness will become the only driving force if all the particles are spherical. To validate this, glass particles with different roughness degrees were produced by conducting abrasion and etching processes for different time scales. In this context, flotation characteristics were investigated in two different systems. First of all, methylated spherical but rough particles were monitored through flotation tests. In these tests, significant increases were obtained with rougher particles in terms of flotation rate constants. These findings in turn clearly suggested that roughness has a pronounced role on the flotation of spherical particles where similar tendencies were also obtained in glass-quartz-amine systems. Aside from these findings, the influence of roughness on interactions between particles was also modeled using DLVO models with added hydrophobic force component derived from van Oss theory. Although,

different results were obtained by theoretical and experimental assumptions, their intersection point indicates an increase of hydrophobic features of particles which lowers the energy barrier between particles and hence increase the flotation recovery. The third sub-hypothesis of this study was isolation of roughness from shape factor on interpreting the flotation results. To validate this, coarse sized spherical glass particles were ground in a controlled process in order to observe the changes on average shape factor and roughness as a function of time for the particles in the same size range. Variation of the shape factor of particles as a function of grinding time was for the first time demonstrated. The changes in roundness values continued to a certain grinding time above which negligible changes were obtained. The ground particles were submitted to an abrasion process with silicon carbide to produce particles with different roughness degrees. In these series of tests, aside a negligible difference on shape factor, particles with different roughness degrees were produced.

Thus, micro-flotation tests performed at different collector dosages showed that the characteristics of the flotation recovery values became a function of roundness values for ground particles while it became a function of roughness for abraded particles. These findings in turn clearly suggested that flotation of particles can well be explained in terms of particle morphology. More importantly, it is shown that while the effect of shape factor is most significant at high collector dosages, that of roughness diminishes at high level of hydrophobicity.

All these results of micro-flotation tests confirmed that particle morphology can be the controlling factor for a successfull flotation for both model and real systems. However, the morphology analysis is still an off-line laboratory technique which needs further development for practical applications.

REFERENCES

Adak, A., Pal, A. (2005). Adsorption of Anionic Surfactant on Alumina and Reuse of the Surfactant-Modified Alumina for the Removal of Crystal Violet from Aquatic Environment. Journal of Environmental Science and Health Part A. *40.* 167-182.

Ahmed, M. M. (2010). Effect of comminution on particle shape and surface roughness and their relation to flotation process. International Journal of Mineral Processing, *94* (3-4):180-191.

Albijanic B., Amini E., Wightman E., Ozdemir O., Nguyen A., Bradshaw D., (2011). A Relationship between the Bubble-Particle Attachment Time and The Mineralogy Of A Copper-Sulphide Ore. Miner. Eng., *24*, 1335-1339, 2011

Albijanic, B., Ozdemir, O., Hampton, M.A., Nguyen, P.T., Nguyen, A.V., Bradshaw, D., (2014). Fundamental aspects of bubble-particle attachment mechanism in flotation separation. Miner. Eng. *65*, 187–195.

Anfruns, J. F., and J. A. Kitchener. (1977). Rate of capture of small particles in flotation. Transactions of the Institute of Mining and Metallurgy, Section C: Mineral Processing & Extractive Metallurgy *86*:9-15.

Bell, G. M., S. Levine, and L. N. McCartney. (1970). Approximate methods of determining r free energy of interaction between two charged colloid spheres. Journal of Colloid and Interface Science *33* (3):335-359.

Bhattacharjee, S., C. H. Ko, and M. Elimelech. (1998). DLVO interaction between rough surfaces. Langmuir *14* (12):3365-3375.

Brunauer, S., Emmet, R.H. and Teller, E. (1938). Adsorption of gases in multimolecular layers. Journal of the American Chemical Society, *62*, 1723-1732.

Chander, S., Hogg, R., (1988). Physical and surface characterization for mineral processing, Minerals and Metallurgical Processing, 152-161.

Chiphunfu, D., Zanin, M., Grano, S., (2011). The dependency of the critical contact angle for flotation on particle size- Modelling the limits of fine particle flotation. Miner. Eng. 24, 51-57.

Dang-Vu, T., Hupka, J., Drzymala, J., (2006). Impact of roughness on hydrophobicity of particles measured by the Washburn method. Physicochemical Problems of Mineral Processing *40*, 45-52.

Derjaguin, B. V. (1934). Untersuchungen uber die reibung und adhasion. IV. Theorie des anhaftens kleiner teilchen (Analysis of friction and adhesion IV. The theory of the adhesion of small particles). Kolloid Zeitschrift *69* (2):155-164.

Djurovic, B. and Jean, E., (1999). Coating removal from fiber composites and aluminium using starch media blasting, Wear, *224*, 22-37.

Drelich, J., and J. D. Miller. (2012). Induction time measurements for air bubbles on chalcopyrite, bornite, and gold in seawater. In Water in Mineral Processing, edited by J. Drelich. Englewood, CO, USA: Society for Mining, Metallurgy, and Exploration, 73-85.

Ducker, W. A., R. M. Pashley, and B. W. Ninham. (1989). The flotation of quartz using a double-chained cationic surfactant. Journal of Colloid and Interface Science *128* (1):66-75.

Feng, D., Aldrich, C., (2000). A comparison of the flotation of ore from the Merensky Reef after wet and dry grinding. Int. J. Miner. Process. *60* (2), 115–129

Fokke, M., (1999). Abrasive Blasting of Metal Surfaces, Delft University Press, Netherlands.

Forssberg E., Zhai H., (1985). Shape and surface properties of particles liberated by autogenous grinding, Scandinavian Journal of Metallurgy, *14*, 25-32.

Fuerstenau, D. W., (1957). Correlation of Contact Angles, Adsorption, Density, Zeta Potentials, and Flotation Rate. Trans. AIME, *208*, 365-367.

Fuerstenau, D.W. and Pradip, (2005). Zeta Potentials in the flotation of oxide and silicate minerals. Advances in Colloid and Interface Science. 114-115. 9-26.

Fuerstenau, D.W., Modi, H.J.,(1959). Streaming Potentials of Corundum in Aqueous Organic Electrolyte Solutions, Journal of the Electrochemical Society, *106*,336-341

Fuerstenau, M. C., G. J. Jameson, and R. H. Yoon. (2007). Froth Flotation: A Century of Innovation. Littleton, CO: Society for Mining, Metallurgy & Exploration.

Guoying, Li, (1998). Surface Engineering. Mechanical Industry Publishing House, Beijing.

Guven, O. Ozdemir, O., Karaagaclioglu, I. E., Celik, M. S., (2014). "Contribution of surface roughness on flotation of glass beads", International Mineral Processing Congress, Chile

Guven, O., Celik, M. S., (2015). Can shape and roughness of particles be tuned to reach maximum flotation recoveries, In: Proceedings of the Flotation ’15. Capetown, South Africa.

Guven, O., Celik, M.S., Drelich, J., (2015). Flotation of methylated roughened glass particles and analysis of particle-bubble energy barrier, Miner. Eng., *79*, 125-132

Guven, O., O. Ozdemir, I. E. Karaagaclioglu, and M. S. Celik. (2015). Surface morphologies and floatability of sand-blasted quartz particles. Minerals Engineering *70*, 1-7.

Hancer, M., and M. S. Celik. (1993). Flotation mechanisms of boron minerals. Separation Science and Technology *28* (9):1703-1714.

Hassas, B.V., Caliskan, H., Guven, O., Karakas, F., Cinar, M., Celik, M.S., (2016). Effect of roughness and shape factor on flotation characteristics of glass beads. Colloids and Surfaces A: Physicochemical and Engineering Aspects *492*, 88-99

Hicyilmaz, C., Ulusoy, U., Bilgen, S., Yekeler, M., Akdogan, G., (2006). Response of rough and acute surfaces of pyrite with 3-D approach to the flotation. Journal of Mining Science, *42* (4): 393-402.

Hiçyılmaz, C., Ulusoy, U., Yekeler, M., (2004). Effects of the shape properties of talc and quartz particles on the wettability based separation processes, Applied Surface Science, *233*, 204-212.

Hoek, E. M. V., and G. K. Agarwal. (2006). Extended DLVO interactions between spherical particles and rough surfaces. Journal of Colloid and Interface Science *298* (1):50-58.

Hoek, E. M. V., S. Bhattacharjee, and M. Elimelech. (2003). Effect of membrane surface roughness on colloid-membrane DLVO interactions. Langmuir *19* (11):4836-4847.

Holt, C. B. (1981). The shape of particles produced by comminution - a review. Powder Technology *28* (1):59-63.

Jianxin, D. and Taichiu, L., (2000). Techniques for improved surface integrity and reliability of machined ceramic composites. Surface Engineering, *16*, 411-414.

Karakas, F., Hassas, B. V., (2016). Effect of surface roughness on interaction of particles flotation. Physicochemical Problems of Mineral Processing. *52*, 18-34.

Koh, P.T.L., Hao, F.P., Smith, L.K., Chau, T.T., Bruckard, W.J., (2009). The effect of particle shape and hydrophobicity in flotation. Int. J. Miner. Process *93*, 128-134.

Krasowska, M. and Malysa, K., (2007). Wetting films in attachment of the colliding bubble. Advances in Colloid and Interface Science, 134-135: 138-150.

Krasowska, M., and K. Malysa. (2007). Kinetics of bubble collision and attachment to hydrophobic solids: I. Effect of surface roughness. International Journal of Mineral Processing *81* (4):205-216.

Kursun, H., Ulusoy, U., (2006). Influence of shape characteristics of talc mineral on the column flotation behavior. Int. J. Miner. Process, *78*, 4, 262-268

Lange, D. A., Jennings, H. M. and Shah, S.P., (1993). Analysis of surface roughness using confocal microscopy, Journal of Materials Science, *28*, 3879-3884.

Laskowski, J. S., Z. Xu, and R. H. Yoon. (1991). Energy barrier in particle-to-bubble attachmet and its effect on flotation kinetics. Paper read at XVIIth International Mineral Processing Congress, at Dresden, Germany, Sept. 23-28, 1991.

Laskowski, J.S., Vurdela, R.M. and Liu, Q., (1988). The colloid chemistry of weak electrolyte- collector flotation. In: K.S.E. Forssberg (Editor), In proceedings of 16th International Mineral Processing Congress, 703-715.

Leica QW in User Manual, (1995). Leica Q500MC QWin User Manual.

Little, L., Becker, M., Wiese, J., Mainza, A. N., (2015). Auto-SEM particle shape characterization: Investigating fine grinding of UG2 ore. Miner. Eng., *82*, 92-100.

Mahmoud, M., A., (2010). Effect of comminution on particle shape and surface roughness and their relation to flotation process. International Journal of Mineral Processing. *94*, 180-191

Medalia, A.I., (1980). Three-dimensional shape parameters. In:Beddow, J.K., Meloy, T. (Eds.), Testing and Characterization of Powders and Fine Particles. Heyden, London, pp. 66- 76.

Meloy, T.P., Williams, M.C., (1994). Particle shape characterization, new and old methods: Does a particle have shape. Challenges in Mineral Processing, pp. 207-221. Chapter 12

Modi, H.J., Fuerstenau, D.W.,(1960) The Flotation of Corundum-An Electrochemical Interpretation. Trans. AIME, *217*, 381-387

Nguyen, A. V., J. Drelich, M. Colic, J. Nalaskowski, and J. D. Miller. (2007). Bubbles: interaction with solid surfaces. In Encyclopedia of Surface and Colloid Science, edited by P. Somasundaran. London: Taylor & Francis, 1-29.

Oliver, J.F., Huh, C., Mason, S.G., (1980). An experimental study of some effects of solid surface roughness on wetting, Colloids and Surfaces, *1*, 79-104.

Ozdemir, O. (2013). Specific ion effect of chloride salts on collectorless flotation of coal. Physicochemical Problems of Mineral Processing *49* (2):511-524.

Pineres, J., and J. Barraza. (2011). Energy barrier of aggregates coal particle-bubble through the extended DLVO theory. International Journal of Mineral Processing *100* (1-2):14-20.

Ralston, J., S. S. Dukhin, and N. A. Mishchuk. (2002). Wetting film stability and flotation kinetics. Advances in Colloid and Interface Science *95* (2-3):145-236.

Rezai, M., Rahimi, M., Aslani, M.R., Eslamian A. and Dehghani, F., (2010). Relationship between surface roughness of minerals and their flotation kinetics, Proceedings of the XI International Seminar on Mineral Processing Technology, Editors: R. Singh, A. Das, P.K. Banerjee, K.K. Bhattacharyya and N.G. Goswami, pp. 232-238.

Sarkar, N., Chaudhuri, B.B., (1994). An efficient differential box counting approach to compute fractal dimension of image. IEEE Transactions on Systems, Man. And Cybernetics, 24 Jan.

Schmidt, D. C., and J. C. Berg. (1996). The effect particle shape on the flotation of toner particles. Progress in paper Recycling *5* (2):67-77.

Singh, P., Ramakrishnan, P., (1996). Powder characterization by particle shape assessment. KONA, *14*, 16-30.

Sun, N., and J. Y. Walz. (2001). A model for calculating electrostatic interactions between colloidal particles of arbitrary surface topology. Journal of Colloid and Interface Science *234* (1):90-105.

Suresh, L. and J. Y. Walz. (1997). Direct measurement of the effect of surface roughness on the colloidal forces between a particle and flat plate. Journal of Colloid and Interface Science *196* (2):177-190.

Suresh, L., and J. Y. Walz. (1996). Effect of surface roughness on the interaction energy between a colloidal sphere and a flat plate. Journal of Colloid and Interface Science *183* (1):199-213.

Szleifer, I., Shaul, A.B., Gelbert, W.M., (1986). Chain statistics in micelles and bilayers: effects of surface roughness and internal energy. Journal of Chemical Physics, *85*(9), 5345-5358.

Ulusoy, U. (1996), Effect of shape characteristics of particles on floatability, MSc. Thesis, METU, Ankara, Turkey.

Ulusoy, U. and Kursun, I., (2011). Comparison of different 2D Image Analysis measurement techniques for the shape of talc particles produced by different media milling. Minerals Engineering, *24*, 91-97.

Ulusoy, U. Yekeler, M., (2005). Correlation of the surface roughness of some industrial minerals with their wettability parameters. Chem. Eng. Process. *44*, 557-565

Ulusoy, U. Yekeler, M., Hiçyılmaz, C., (2003). Determination of the shape, morphological and their wettability properties of quartz and their correlations. Miner. Eng., *16*- 951-954.

Ulusoy, U., and M. Yekeler. (2014). Dynamic image analysis of calcite particles created by different mills. International Journal of Mineral Processing *133*:83-90.

Ulusoy, U., Hicyilmaz, C., Yekeler, M., (2003). Role of shape properties of calcite and barite particles on apparent hydrophobicity. Chemical Engineering and Processing, *43*, 1047-1053.

Ulusoy, U., Yekeler, M., (2004). Variation of critical surface tension for wetting of minerals with roughness determined by Surtronic 3+ instrument. International Journal of Mineral Processing, *74*, 61-69.

van Oss, C. J. (1994). Interfacial Forces in Aqueous Media. New York: Marcel Dekker, Inc.

Verelli, D.I., Bruckard, J. W., Koh, L. T. P., Schwarz, P., M.and Follink, B., (2014). Particle shape effects in flotation. Part 1: Microscale experimental observations, Minerals Engineering, *58*, 80-89.

Verelli, D.I., Koh, P.T.L., Nguyen, V.A., (2011). Particle-bubble interaction and attachment in flotation. Chemical Engineering Science. *66*, 5910-5921.

Vizcarra, T.G., Harmer, S.L., Wightman, E. M., Johnson, N.W., Manlapig, E.V., (2010). The effect of breakage mechanism on the mineral liberation properties of sulphide ores Miner. Eng. *23*, 374-382.

Vizcarra, T.G., Harmer, S.L., Wightman, E. M., Johnson, N.W., Manlapig, E.V., (2011). The influence of particle shape properties and associated surface chemistry on the flotation kinetics of chalcopyrite. Miner. Eng. *24*, 807-816.

Walz, J. Y., L. Suresh, and M. Piech. (1999). The effect of nanoscale roughness on long range interaction forces. Journal of Nanoparticle Research 1 (1):99-113.

Wiese, J., Becker, M., Yorath, G., O'Connor, C., (2015). An investigation into the relationship between particle shape and entrainment. Miner. Eng., *83*, 211-216.

Yekeler, M., Ulusoy, U., Hiçyılmaz, C., (2004). Effect of particle shape and roughness of talc mineral ground by different mills on the wettability and floatability. Powder Technology. *140* (1-2). 68-78.

Yoon, R. H., and L. Q. Mao. (1996). Application of extended DLVO theory .4. Derivation of flotation rate equation from first principles. Journal of Colloid and Interface Science *181* (2):613-626.

Yoon, Roe-Hoan and Yordan, Jorge L., (1990). Induction Time Measurements for the Quartz-Amine Flotation System. Journal of Colloid and Interface Science, *141*, 374-382.

Yoon, Roe-Hoan., (2000). The Role of Hydrodynamic and Surface Forces in Bubble/Particle Interaction, Int. J. Miner. Process, *58* (1-4). 129-143

Zisman, W.A., (1964). Relation of Equilibrium Contact Angle to Liquid and Solid Constitution in Contact Angle, In: Gould, R.F., (Ed.), Wettability and Adhesion, Advances in Chemistry Series No. 43. American Chem. Soc. pp. 1–51.

CURRICULUM VITAE

Name Surname **:** Onur GÜVEN

Place and Date of Birth **:** Mersin, Nov 20 1984

E-Mail **:** oguven@itu.edu.tr

EDUCATION

- **B.Sc. :** 2006, Cukurova University, Faculty of Engineering and Architecture, Mining Engineering Department
- **M.Sc. :** 2010, Istanbul Technical University, Faculty of Mines, Mineral Processing Engineering Department

PROFESSIONAL EXPERIENCE AND REWARDS:

- 2014 TUBITAK 2214A Scholarship for PhD Studies in USA

PUBLICATIONS, PRESENTATIONS AND PATENTS ON THE THESIS:

- **O. Guven**, O. Ozdemir, I. E. Karaagaclioglu, M.S. Çelik, (2105) "Surface morphologies and floatability of sand-blasted quartz particles", Minerals Engineering, *70*, 1-7
- **Onur Guven**, Mehmet S. Celik, Jaroslaw W. Drelich, (2015) "Flotation of methylated roughened glass particles and analysis of particle-bubble energy barrier", Minerals Engineering, *79*, 125-132.

- **Onur Guven**, Mehmet S. Celik, (2016) "Interplay of particle shape and surface roughness to reach maximum flotation efficiencies depending on collector concentration", Mineral Processing and Extractive Metallurgy Review, Accepted.

- **Onur Guven**, Fırat Karakas, Nurgul Kodrazi, Mehmet S. Celik, (2016) "Dependence of morphology on anionic flotation of alumina", International Journal of Mineral Processing. Accepted.

OTHER PUBLICATIONS, PRESENTATIONS AND PATENTS:

- **O. Guven**, F. Karakas, M. A. Kaya, H. Yildirim, M. S. Celik, "Composite Films Based on Styrene-Co-Butyl-Acrylate With Colemanite and Calcium Bentonite Mineral Fillers", Mechanics of Composite Materials, Vol. 3, No. 50, 07/2014, ISSN: 0191-5665,
- Feridun Boylu, Tan Cetinel, **Onur Guven**, Fırat Karakas, Kenan Cinku, İbrahim Ethem Karaağaçlıoğlu, Mehmet Sabri Celik, "Optimum Separation Route For Semi Bituminous Coal Using Semi-Plot Scale Pneumatic Stratification Jig", Physicochemical Problems of Mineral Processing, Vol. 51, No. 2, 01/2015, s. 559-573, ISSN: ISSN 2084-4735
- F. Boylu, K. Çinku, T. Çetinel, F. Karakaş, **O. Güven**, İ.E. Karaağaçlıoğlu, M.S. Çelik, "Effect of Coal Moisture on the Treatment of a Lignitic Coal Through a Semi-Pilot Scale Pneumatic Stratification Jig", International Journal of Coal Preparation and Utilization, 01/2015
- Behzad Vaziri Hassas, Hidayet Caliskan, **Onur Guven**, Fırat Karakas, Mustafa Cınar and Mehmet S. Celik, "Effect of Roughness and Shape Factor on Flotation Characteristic of Glass Beads" Colloids and Surfaces A Physicochemical and Engineering Aspects, 2016, 492, 88-99
- **Onur Güven**, Behzad Vaziri Hassas, İbrahim Ethem Karaağaçlıoğlu, Fırat Karakaş, Mehmet Sabri ÇELİK, "Kolemanit ve Bentonit Katkılı Stiren Bütil Akrilat Kopolimer bazlı kompozit Üretimi ve Karakterizasyonu", Boya Turk, No. 01/ 2, 01/2014
- Ekrem Yüce, Mustafa Özer, **Onur Güven**, "Avrupa ve Türkiye Kömür Endüstrisi Enerji Üretim Verileri", Madencilik Türkiye, No. 40, 07/2014, s. 90-100, ISSN: 1309-1670, Madencilik ve Yer Bilimleri Dergisi
- **Onur Güven**, Fırat Karakaş, Gökhan Yaşar, Mehmet S. Çelik, "Morphological Character and Floatability of Blasted Talc Particles", International Journal of Mining, Materials and Metallurgical Engineering, Vol. 1, No. 1, 12/2015, s. 11-15, ISSN: TBD, Avestia Publishing
- F. Karakaş, G. Güldan, G. Ersever, İ. Erkan, **O. Güven**, M. S. Çelik, "Use of Industrial Raw Materials in Paint Production", 01/2009, s. 416-424, 7th International Industrial Raw Materials Symposium and Exhibiti, Kuşadası, 25.02.2009 - 27.02.2009
- **O. Güven**, M. A. Kaya, H. Yıldırım, M. S. Çelik, "Preparation and Characterization of Styrene Butyl Acrylate and Calcium Bentonite Nanocomposite", 06/2009, s. 306-309, Proceedings of the XIII Balkan Mineral Processing Congress, Romania, 14.06.2009 - 17.06.2009

- **O. Güven**, M. S. Çelik, "Composite Materials Based on Styren Butile Acrylate and Colemanite: Preparation and Characterisation", 12/2009, Processing of Industrial Minerals'09, Istanbul, 04.02.2010 - 05.02.2010
- **O. Güven**, G. Bulut, N. Durmaz, O. Kangal, F. Arslan, "Concentration of Phosphate Ore by Flotation With/Without Desliming", 09/2010, s. 1911-1916, XXV International Mineral Processing Congress-IMPC 2010, Avustralia-Brisbane, 06.09.2010 - 10.09.2010
- **O. Güven**, M. A. Kaya, H. Yıldırım, M. S. Çelik, "Preparation of Composite Materials with Colemanite Additive on Styrene Butyl Acrylate Copolymer Latexes", 09/2010, s. 292-297, PaintIstanbul, Istanbul, 24.09.2010 - 25.09.2010
- **O. Güven**, F. Burat, G. Bulut, G. Önal, "Evaluation of Lead-Zinc Ore Tailings by Flotation", 10/2010, s. 415-420, Proceedings of XII th International Mineral Processing Symposium, Cappadocia, Turkey, 06.10.2010 - 08.10.2010
- **O. Güven**, G. Bulut, K. T. Perek, "Effect of shape factor on coal flotation", 10/2010, s. Cd Proceeding, Twenty-Seventh Annual International Pittsburg Coal Conference, Istanbul, 11.10.2010 - 14.10.2010
- **O. Güven**, F. Burat, O. Kangal, N. Acarkan, G.Önal, "Beneficiation of Antimony Tailings", 06/2011, s. 769-772, XIV Balkan Mineral Processing Congress 2011, Bosnia Herzegovina- Tuzla, 14.06.2011 - 16.06.2011
- **O. Güven**, B. Even, G. Bulut, A. E. Yüce, "Enrichment of Disseminated Copper Ores by Flotation Method", 10/2012, s. 341-348, Proceedings of XIII th International Mineral Processing Symposium, Bodrum, 10.10.2012 - 12.10.2012
- **O. Güven**, C. Küçüktaş, A. Gül, "Optimization of Shaking Table for Beneficiation of Chromite Ore", 10/2012, s. 187-190, XIII. International Mineral Processing Symposium, Bodrum, 10.10.2012 - 12.10.2012
- **O. Güven**, S. Kara, M. Özer, M. O. Kangal, "Beneficiation of Carbonaceous Phosphate Ores", 11/2012, s. Cd Proceeding, 8. Uluslararası Endüstriyel Hammaddeler Sempozyumu, İstanbul, 29.11.2012 - 30.12.2012
- F. Karakaş, **O. Güven**, M. Müdüroğlu, M. S. Çelik, "Separation of Lime from Petroleum Coke in Lime Furnace Flue Dust", 10/2012, XIII International Mineral Processing Symposium, Bodrum, 10.10.2012 - 12.10.2012
- B. Kocabaş, **O. Güven**, M. Özer, M. O. Kangal, "The Beneficiation of Antimony Ore by Flotation", 2014, s. 207-210, XIII International Mineral Processing Symposium, Bodrum, 10.10.2012 - 12.10.2012
- B. Vaziri Hassas, **O. Güven**, F. Karakaş, M. S. Çelik, "Recovery of Petroleum Coke from Lime Calcinations Process Tailings", 06/2013, s. 309-313, XV Balkan Mineral Processing Congress 2013, Sozopol, Bulgaria, 12.06.2013 - 16.06.2013
- F. Boylu, K. Çinku, T. Çetinel, **O. Güven**, N. Yalçın, M. S. Çelik, "Dry Processing of -4 mm Coal Fines Through Air Jig and Aerodynamic Separator", 2014, s. 541-546, XV Balkan Mineral Processing Congress 2013, Sozopol, Bulgaria, 12.06.2013 - 16.06.2013
- N. Coşkun, B. Aydın, **O. Güven**, İ. Eriş, B. Benli, "Recovery of Fine Abrasive Garnet from The Resotration of Historical Buildings Wastes", 2014, s. 1063-1066, XV Balkan Mineral Processing Congress 2013, Sozopol, Bulgaria, 12.06.2013 - 16.06.2013

- **O. Güven**, B. Vaziri Hassas, F. Karakaş, "The Usage of Sodium Bentonite in Styrene Butyl Acrylate Composites", 2014, s. 1157-1159, XV Balkan Mineral Processing Congress 2013, Sozopol, Bulgaria, 12.06.2013 - 16.06.2013
- F. Karakaş, B. Vaziri Hassas, **O. Güven**, M. S. Çelik, "Utilization of Colemanite in Water Borne Paints As a Filler and Fire Retardant", 06/2013, s. 1235-1238, XV Balkan Mineral Processing Congress 2013, Sozopol, Bulgaria, 12.06.2013 - 16.06.2013
- G. Ateşok, **O. Güven**, M. Kılıç, M. Özer, "The Future of Renewable Energy Sources", 2014, s. 1239-1242, XV Balkan Mineral Processing Congress 2013, Sozopol, Bulgaria, 12.06.2013 - 16.06.2013
- Ö. F. Ersoy, H. Turgut, **O. Güven**, K. Çinku, O. Kökkılıç, O. Özdemir, "Effect of Heat Treatment on the Flotation of Turkish Lignites in Brine Solution", 10/2013, s. Cd Proceeding, Materials Science & Technology 2013, Canada, Montreal, Quebec, 27.10.2013 - 31.10.2013
- B. V. Hassas, F. Karakas, **O. Güven**, M. S. Celik, "Effect of hydrophilic lipophilic balance (HLB) of nonionic surfactants on ultrafine lignite dewatering", 10/2014, International Mineral Processing Congress, Chile, 20.10.2014 - 24.10.2014
- **O. Güven**, O. Ozdemir, I. E. Karaagaclioglu, M. S. Celik, "Contribution of surface roughness on flotation of glass beads", 10/2014, International Mineral Processing Congress, Chile, 20.10.2014 - 24.10.2014
- O. Kangal, S.Kara, U.Çınar, **O. Güven**, "Effects of Different Parameters on Phosphate Flotation", 10/2014, International Mineral Processing Symposium 2014,Kuşadası